

The University of Maine

DigitalCommons@UMaine

Electronic Theses and Dissertations

Fogler Library

Spring 5-5-2023

Investigation into Sintered Lunar Regolith Construction Methods and Novel Usability Evaluation

Thomas A. Cox

University of Maine, thomas.cox@maine.edu

Follow this and additional works at: <https://digitalcommons.library.umaine.edu/etd>



Part of the [Other Mechanical Engineering Commons](#), [Space Habitation and Life Support Commons](#), and the [Structures and Materials Commons](#)

Recommended Citation

Cox, Thomas A., "Investigation into Sintered Lunar Regolith Construction Methods and Novel Usability Evaluation" (2023). *Electronic Theses and Dissertations*. 3794.

<https://digitalcommons.library.umaine.edu/etd/3794>

This Open-Access Thesis is brought to you for free and open access by DigitalCommons@UMaine. It has been accepted for inclusion in Electronic Theses and Dissertations by an authorized administrator of DigitalCommons@UMaine. For more information, please contact um.library.technical.services@maine.edu.

**Investigation into Sintered Lunar Regolith Construction Methods and Novel Usability
Evaluation**

By

Thomas Cox

B.A. University of Maine, 2020

M.A. University of Maine, 2023

A Thesis

Submitted in Partial Fulfillment of the

Requirements for the Degree of

Master of Science

(in Mechanical Engineering)

The Graduate School

The University of Maine

May 2023

Advisory Committee:

Justin Lapp, Assistant Professor of Mechanical Engineering, Advisor

Senthil Vel, Professor of Mechanical Engineering

Bashir Khoda, Associate Professor of Mechanical Engineering

© 2023 Thomas Cox

All Rights Reserved

Investigation into Sintered Lunar Regolith Construction Methods and Novel Usability Evaluation

By Thomas Cox

Thesis Advisor: Dr. Justin Lapp

An Abstract of the Thesis Presented
in Partial Fulfillment of the Requirements for the
Degree of Master of Science
(in Mechanical Engineering)
May 2023

Since the Apollo missions in the late 1960's, there has been a growing interest shared by many countries around the world to return to the Moon and establish a permanent Lunar settlement. The first phase of temporary Lunar bases will be established over the next several years. For a permanent human presence on the Moon, it will be necessary to use locally available resources for the construction of Lunar habitats and other infrastructure. Sintering Lunar regolith has been shown to be a promising method for producing structural material with a variety of desirable properties from strength to radiation shielding. While many experiments have been done to develop new methods of sintering, little progress has been made on producing usable construction material. Furthermore, a wide variety of sintering methods have been proposed which represent a range of strengths and weaknesses.

This research aims to fill a gap in the existing literature with regard to evaluating the characteristics of usable sintered regolith and the performance of associated sintering methods in the context of selecting a suitable method for early Lunar development. A literature review was conducted to investigate existing sintering methods and to define the most important parameters relating to usability. This information was used to compile the Usability Criteria, a novel

evaluation tool for comparing sintering methods and their products across seven fundamental categories. For sintered bricks or structural material; strength, hardness, and uniformity are considered. Sintering methods and equipment are assessed based on energy efficiency, versatility, labor requirement, and a combination of production rate and mass efficiency. Four grade levels were designated within each criterion as well as an overall importance factor ranging from 1-5. Two promising sintering methods, selected for their unique processes and resulting products, were then reproduced at laboratory scale to make bricks from Lunar regolith simulant.

The first method made use of a high-temperature furnace and custom molds to make bricks using radiant heating. The second method involved forming bricks by applying consecutive thin layers of regolith on top of one another in between periods of concentrated solar radiation exposure. Data was collected from the sintered bricks as both a contribution to the existing body of sintered regolith research and for evaluation under the Usability Criteria. Considering that the Usability Criteria are intended for full-scale sintering system evaluation, the numerical scores applied to the laboratory-scale systems are only valid for comparison purposes. The furnace-sintered samples performed better in energy efficiency and had a significantly higher average compressive strength. The solar-additive-manufacturing samples outperformed the furnace samples in most system-based categories, particularly in production rate and mass efficiency. While some criteria will likely be adjusted, and others may be added or removed, the proposed evaluation tool may be beneficial in guiding future research and eventually the selection process for Lunar sintering and construction equipment.

DEDICATION

To my mother, for inspiring in me the love of science and supporting me every step of the way.

To my father, for encouraging me to look to the stars.

ACKNOWLEDGEMENTS

I would like to thank my advisor, Dr. Justin Lapp, for encouraging me to pursue higher education. I would also like to recognize the assistance of Diprajit Biswas, Dr. Beverly Kemmerer, Stephen Abbadessa, and Dr. Keith Berube.

Table of Contents

DEDICATION	v
ACKNOWLEDGEMENTS	vi
TABLE OF CONTENTS	vii
LIST OF TABLES	x
LIST OF FIGURES	xi
Chapters	
INTRODUCTION	1
1.1. The Motivation for Space Exploration and Development	1
1.2. Lunar Exploration History	2
1.3. Future Lunar Development Motivation	3
1.3.1. Lunar Resource Extraction	4
1.3.2. Private Space Initiatives	5
1.3.3. Beyond the Moon	6
1.4. Establishing a Lunar Base	8
1.5. ISRU	11
1.6. Research Objectives	12
LUNAR REGOLITH FOR CONSTRUCTION	14
2.1. Lunar Regolith	14
2.2. Regolith Simulants	15
2.3. Uses of Lunar Regolith	17
2.4. Regolith Sintering	19
2.4.1. Furnace Sintering	21
2.4.2. Concentrated Solar Sintering	22

2.4.3. Microwave Sintering	23
2.4.4. Additive Manufacturing	25
USABILITY CRITERIA	27
3.1. Usability Criteria Overview	27
3.2. Compressive Strength	28
3.3. Hardness.....	31
3.4. System Versatility.....	33
3.5. Energy Cost per Unit Volume.....	35
3.6. Labor Requirement	38
3.7. Brick Uniformity.....	40
3.8. Production Rate and Mass Efficiency.....	41
EXPERIMENTAL METHODS AND RESULTS.....	46
4.1. Methods.....	46
4.2. Lunar Highlands Simulant	46
4.3. Furnace Sintering: Furnace Setup	47
4.3.1. Furnace Sintering: Initial Trials	48
4.4. Solar AM: Solar Simulator Setup	49
4.4.1. Solar AM: Test Stand Design	50
4.4.2. Solar AM: Initial Trials	51
4.5. Brick Sample Processing	54
4.6. Strength Testing Procedure.....	56
4.7. Compressive Strength Results	59
4.8. Elasticity Calculation	61
4.9. Compressive Strength Consistency in Prior Research.....	62
APPLIED USABILITY CRITERIA.....	64

5.1. Method Usability Evaluation	64
5.2. Sample Grading and Discussion	64
5.2.1. Compressive Strength	66
5.2.2. System Versatility	67
5.2.3. Energy Cost per Unit Volume	68
5.2.4. Labor Requirement.....	70
5.2.5. Production Rate and Mass Efficiency	71
5.3. Matrix Evaluation	73
CONCLUSION AND FUTURE WORK	75
6.1. Conclusion	75
6.2. Future Work	76
BIOGRAPHY OF THE AUTHOR.....	90

LIST OF TABLES

Table 1	Usability Criteria importance factors and descriptions.....	28
Table 2	List of Usability Criteria with weights	28
Table 3	Compressive strength grading parameters	31
Table 4	Energy requirement grading parameters.....	37
Table 5	Production rate levels.....	45
Table 6	Mass efficiency grading parameters	45
Table 7	Furnace sintering test experiment data	59
Table 8	Final furnace-sintered brick measurements	60
Table 9	Final solar-AM sintered brick measurements	61
Table 10	Average compressive strengths, strength standard deviations, and average Young's moduli per method	62
Table 11	Usability Criteria score matrix.....	74

LIST OF FIGURES

Figure 1	Artistic rendition of NASA’s Artemis Lunar Base	8
Figure 2	Artistic rendition of NASA’s Inflatable Lunar Base Concept.....	9
Figure 3	Example of Lunar Regolith mineral composition via X-ray diffraction	15
Figure 4	In-house sintered Lunar brick sample (LHS-1 simulant)	19
Figure 5	Furnace-sintered cylindrical bricks	21
Figure 6	Regolith simulant slabs sintered with concentrated solar light	22
Figure 7	Microwave-sintered samples of regolith simulant	23
Figure 8	ESA’s hollow closed-cell concrete structure 3D-printed simulating regolith characteristics	33
Figure 9	Artistic rendition of ICON’s Lunar additive manufacturing technology	38
Figure 10	Silicon carbide mold containing regolith simulant.....	47
Figure 11	Lightly-sintered test sample	48
Figure 12	Solar simulator experimental setup	49
Figure 13	Exploded view of the mirror housing and water-cooling system.....	50
Figure 14	Crucible containing irradiated regolith simulant (left) and cooled, sintered regolith simulant (right)	52
Figure 15	Test sample composed of 8 regolith simulant layers.....	53
Figure 16	Furnace-sintered bricks samples.....	54
Figure 17	Solar-AM sintered brick samples	55
Figure 18	Representative final furnace sample load vs. deflection curve	56
Figure 19	Representative test furnace sample load vs. deflection curve	57
Figure 20	Representative final solar-AM sample load vs. deflection curve.....	58

Figure 21 Truncated load-deflection curves with linear-elastic slope approximations61

CHAPTER 1

INTRODUCTION

1.1. The Motivation for Space Exploration and Development

It is widely understood that sustained survival of the human species must involve interplanetary colonization. Cosmic threats such as meteoroids and solar flares and impending issues on Earth such as the climate crisis and overpopulation make it essential for humans to become an interplanetary species. An important intermediate step in this direction involves exploration and settlement of our closest celestial neighbor, the Moon [1]. At least 22 Lunar missions have been conducted since the Apollo program in the 1960s, and with new developments in reusable rocket technology the financial barrier is decreasing rapidly. Exploration of the Moon gives humans insight into the origins of our own planet as well as information useful for future endeavors beyond. Due to the difficulty of escaping Earth's gravitational field and atmosphere, missions aimed farther into the solar system would greatly benefit from refueling infrastructure on the Moon, such as NASA's Gateway project [1]. Furthermore, establishing a permanent Lunar settlement will allow for extensive study of the moon ultimately leading to significant scientific, political, and economic gain. Permanent settlement will require substantial resources to establish the necessary infrastructure which may include habitats, landing pads, bridges, berms, and roads [2]. Humans will face many challenges during colonization including safety, energy production, and resource management [3] [4].

1.2. Lunar Exploration History

During the late 1950's, in the midst of the Cold War, the United States and the Soviet Union began the first series of missions aimed at the Moon in what was largely a political showdown. The US's first four and the USSR's first seven launches were characterized by catastrophic rocket failure. In 1959, the US's Pioneer 4 achieved the first successful Lunar flyby, followed by the USSR's first Lunar impactor by Luna 2. Each nation experienced a series of further mission failures until 1966 when the USSR's Luna 9 became the first spacecraft to make a successful controlled landing on the Moon. Over a dozen other Lunar missions were conducted with varying levels of success, ranging from orbital satellites to Lunar rovers and sample return missions [5]. The legacy of this early generation of Lunar exploration is of course dominated by the triumphant success of the Apollo missions and the first human exploration of the Lunar surface in 1969. Harrison H. Schmitt, Apollo 17 astronaut, writes in his book Return to the Moon, "A great beneficiary of Apollo has been and continues to be the science of the Earth, the planets, and the solar system. From the samples collected and placed in context by the astronauts, there came a first-order understanding of the origin and history of the Moon" [6]. In 1990, Japan launched its first Lunar spacecraft, followed by the European Space Agency in 2006, China in 2007, and India in 2008. The primary goal of these missions was to gather Lunar mapping and reconnaissance information and to test and develop new technology [5].

While benefits such as scientific discovery and economic gain are motivating factors, there is undoubtedly a far deeper attraction to the endeavor of space exploration. A central tenet of our species seems to be the assertion that we are free to migrate, explore, and expand. Schmitt writes, "One possible view of the future of humankind consists of a positive, expansive continuum – the "Star Trek" vision. That of human migration into new habitats and the

perpetuation of our search for new opportunities, personal fulfillment, and freedom.” Space has surely captured our imaginations for hundreds of thousands of years, but only for the last 50 years has this final frontier occupied the collective zeitgeist as a possible new realm for human migration and exploration. Schmitt continues, “Apollo also accelerated improvements in the human condition for billions of people on Earth. Its success gave hope to people world wide, as demonstrated by the reactions of those millions lining streets to see astronauts and cosmonauts on their world tours.” The global reverberation of such an astonishing achievement has left a legacy of political support for space development in the United States and governments around the world.

1.3. Future Lunar Development Motivation

The motivation for Lunar exploration and development has evolved over time, beginning during the space race of the late 1950’s as a predominantly political challenge, during the late 20th century as a period of scientific discovery, and during the 21st century as an expansion of human activity beyond Earth. A considerable component of this motivation to return to the moon and to continue funding space exploration today is collateral technological development. Schmitt writes, “the technological foundations expanded by, or because of, Apollo, have revolutionized the world’s use of communications, computers, medical diagnostics and care, transportation, weather and climate forecasting, energy conversion systems, new materials, systems engineering, project management, and many other applications of human ingenuity.” Tackling a challenge such as landing a human on the moon requires an immense technological push, which, in the process, benefits nearly every adjacent scientific field. Of course, humans have already landed on the Moon. The next challenge which promises collateral technological development is the

establishment of a permanent human presence on the Moon. A Lunar base would not only provide significant scientific benefits, but it would serve as a catalyst for the development of space industries, the discovery and use of Lunar resources, and the expansion of human settlement to other bodies beyond the Moon.

1.3.1. Lunar Resource Extraction

As stated in a Space Policy editorial in 2016, “To date, all human economic activity has depended on the material and energy resources of a single planet, and it has long been recognized that developments in space exploration could in principle open our closed planetary economy to external resources of energy and raw materials.” Furthermore, it states that “[Lunar resources] ...may permit the construction and operation of scientific facilities in space that would be unaffordable if all the required material and energy resources had to be lifted out of Earth’s gravity. Examples may include the next generation of space telescopes, sample return missions to the outer solar system, and human research stations on the Moon and Mars” [7]. Few resources found on the Moon are likely viable for export to Earth, but one often suggested as a potential clean energy source in fusion reactors is Lunar Helium-3 [6] [8] [9]. Minerals, metals, and compounds such as water can be found in Lunar regolith, as discussed in section 3.2. Early Lunar settlement will take advantage of these resources, such as extracting ice for oxygen production, but establishing a permanent base will expand our ability to use these resources. Eventually, Lunar facilities will be capable of manufacturing tools, advanced materials, and even rocket components and fuel from resources on the Moon [10]. Many studies have explored the economic viability of Lunar resource extraction [1] [3] [4] [11] [7].

1.3.2. Private Space Initiatives

Recently, the private space industry has proven itself as a considerable force in technological achievement, most notably reusable rocket technology whose best example is SpaceX's Falcon 9. America is known for its investor-driven, free market economy. This makes it the perfect environment for a new, intranational space race. Private companies such as SpaceX, Boeing, and Blue Origin are competing for public government contracts aiming to deliver the best and most advanced space technology. Several companies, including Virgin Galactic, have begun to open the space tourism industry, offering flights to the edge of space. In May of 2020, SpaceX became the first private company to send humans into space, and the company has had 207 successful launches at the time of writing, proving that the private sector is capable of competing with government institutions in the space enterprise [12].

Over the past couple of decades, a variety of startup companies have emerged with hopes of paving the first paths into the Lunar and asteroid mining industries. California-based AstroForge is a company who recently announced its ambition to mine platinum-group metals such as palladium – which has a high market demand on Earth – from asteroids [13]. Lunar Resources, Inc. is a space industrial company with the goal of accelerating space manufacturing and resource extraction. Proposed Lunar projects include a radio observatory on the far side of the Moon, large-scale Lunar power grids, and high-efficiency regolith additive manufacturing technology [14]. Lunar Outpost is another Lunar development company making a significant impact in the exploration and mobility space. They recently partnered with Northrup Grumman to help develop a new Lunar Terrain Vehicle (LTV) for NASA's Artemis missions. Furthermore, they aim to land the first rover at the Lunar south pole in 2023, helped develop the first

successful system for making oxygen on Mars, and designed a heavy-weight ice-extraction rover for propellant production [15].

A useful analog for cooperation of national agencies and private companies for Lunar development may be the International Space Station and its private partners. NASA will likely create the first Lunar outpost through Artemis 3, as a government-funded scientific base. Private companies can then partner with NASA by providing infrastructure and technology (such as Lunar Outpost's ice-extraction rover or Lunar Resources' power grids) to accomplish their own goals, similar to how the ISS serves as an orbital base that private companies can provide modules to or demonstrate technology on. The proliferation of a space economy will require significant Lunar infrastructure which the public sector has planned to initiate, and the private sector has committed to expanding.

1.3.3. Beyond the Moon

The Moon is also an essential component in the exploration of celestial bodies farther into the solar system and beyond. Due to the difficulty of transporting mass out of Earth's gravity, the range of future missions further into the solar system will be greatly increased with the ability to refuel either on the Lunar surface or in Lunar orbit. NASA is currently under Presidential orders to land astronauts on Mars by 2033 [16]. Private companies have proposed even more ambitious goals, such as SpaceX which is planning a crewed mission in 2029 [12]. To prepare for the eventual human exploration and settlement of Mars, the Moon will serve as the perfect testing grounds. NASA administrator Jim Birdstine puts it, "We need to learn how to live and work in another world. The Moon is the best place to prove these capabilities and technologies. The sooner we can achieve that objective, the sooner we can move on to Mars."

[16]. While the Moon itself provides significant attraction for exploration and study, its development for the sake of exploration further into the solar system provides a new dimension of motivation.

NASA's Gateway system, part of their Artemis series of missions, will serve as an orbital base: the first piece of necessary infrastructure for Lunar development. As discussed in a 2018 NASA memorandum, Gateway will function as an access point for crewed surface missions, a scientific laboratory, a communications hub for Earth, and a staging point for missions aimed deeper into space [17]. Paul Kessler, an aerospace engineer for the Mars Integration Group, explains that for NASA's proposed Deep Space Transport – which is designed for 1000-day missions to Mars with four crew members – the Gateway will act as a port of exit and entry for Earth. Equipment, fuel, and other supplies will be sent to the Gateway first in its stable near-rectilinear halo orbit (NRHO). Spacecraft such as the Deep Space Transport can be assembled and fueled at the Gateway, potentially by fuel produced on the Moon, before the astronauts' arrival [18]. In the coming decades, spaceflight to the Moon may become as routine as international flights on Earth, at which point human spaceflight to Mars and beyond will become the new frontier. Stable, permanent infrastructure on the Lunar surface will improve the safety and range of future missions.

1.4. Establishing a Lunar Base



Figure 1. Artistic rendition of NASA's Artemis Lunar Base [23]

Establishing a Lunar base is a goal shared by many countries around the world. The United States plans to construct a Lunar base in 2024 (depiction shown in Figure 1), followed by China in 2028 [19]. A permanent presence on the moon would not only allow for considerably longer, if not indefinite scientific studies, but it would also minimize operational costs for all future missions. Landing procedures and equipment would become much simpler and safer with landing pads [20] [21]. Resources such as oxygen and electricity could be produced on the moon via thermochemical reduction of oxides [22] and photovoltaic cells, respectively. With eventual expansion, dozens of specialized personnel could be stationed on the Moon including scientists, engineers, and medical experts.

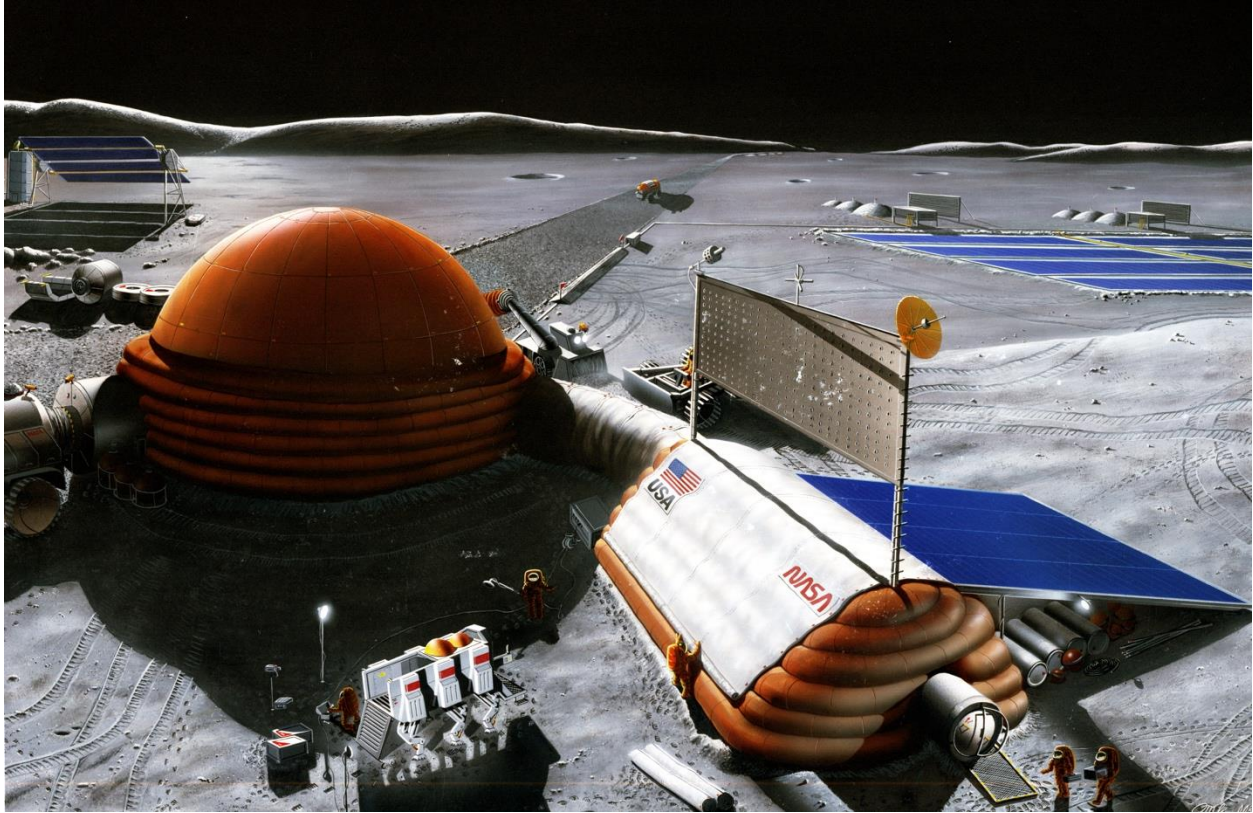


Figure 2. Artistic Rendition of NASA's Inflatable Lunar Base Concept [113]

The initial stages of Lunar surface development will be similar to the development of other extreme environments, such as Antarctica, in that all the necessary survival equipment and supplies will be transported. In 2024, the first Lunar base, established by Artemis 3, will be composed of three main elements: a landing module that also serves as habitation, a lightweight lunar terrain vehicle (LTV), and a pressurized rover that doubles as a mobile habitat [23]. China plans a very similar initial deployment consisting of a lander, hopper, orbiter, and rover [19]. It has been suggested to build complex habitats out of a series of pressurized rovers in a similar manner to the construction of the International Space Station. For at least a century, however, consideration has been given to the wide possibilities of Lunar base architecture. Sub-surface lava tubes have been suggested as a habitat alternative to surface construction [24]. Modern

proposals for initial-stage development often include inflatable structures (shown in Figure 2) which minimize transported mass and maximize habitable volume [25] [26] [27] [28] [29] [30]. Environmental shielding is afforded by an overlay of regolith. A resourceful proposal by King et al. suggests recycling the liquid oxygen tanks of the space shuttle (and theoretically other space craft) as a rudimentary Lunar habitat [31].

The use of lightweight and hybrid habitation units is ideal for early Lunar development but not commensurate with a permanent presence. For long-term Lunar habitation which includes the accommodation of more extensive scientific study and an increasing Lunar population, permanent structures must be built. Necessary structures for a long-term Lunar presence include large habitation units, roads, bridges, landing pads, and berms [32]. Large habitation units provide more accommodating and comfortable living quarters as well as other facilities such as scientific workspace, farming space, and storage. Roads and bridges reduce transportation risk and complexity and increase ease of expansion and breadth of exploration. Landing pads stabilize the surface and greatly reduce the risk associated with take-offs and landings [21]. Simpler structures such as berms and walls can aid in dust and ejecta mitigation around roads and landing pads.

In a review paper entitled “Engineering of lunar bases”, the authors provide a concise summary of the challenges the Lunar environment poses when considering construction, stating

Key environmental factors affecting lunar structural design and construction are:

one-sixth [gravity], the need for internal air pressurization of habitation rated structures, the requirement for shielding against radiation and micrometeorites, the hard vacuum and its effects on some exotic materials, a significant dust

mitigation problem for machines and airlocks, severe temperatures and temperature gradients, and numerous loading conditions—anticipated and accidental. The structure on the Moon must be maintainable, functional, compatible, easily constructed, and made of as much local materials as possible.

[32]

Construction on the Moon presents a combination of challenges never before attempted. The technological advancements required to successfully establish a permanent settlement will likely take decades of work and international cooperation.

1.5. ISRU

In-situ resource utilization (ISRU) is the practice of using locally available resources at one's disposal as opposed to importing resources [1] [3]. The financial and energy costs of transporting resources from the Earth to the Moon and beyond has created a push for ingenuity regarding in-situ solutions. Carpenter et al., in a paper evaluating the viability of Lunar ISRU, states, "If humans are ever going to live and work on the Moon or on Mars in a long-term and sustainable way then dependency on resupply from Earth must be reduced to a minimum or removed completely. To achieve this requires that maximum use is made of any local resources that are available" [7]. Lunar regolith, the fine gray soil comprising the Lunar surface, has been studied for decades and has proven to be a promising resource for colonization [11] [7] [22]. Since the first Lunar samples were returned to Earth by the Soviet Union's Luna 16 [5], a multitude of potential uses for regolith have been explored, including as a construction material, as radiation shielding, for the production of fuels and extraction of useful compounds, elements,

and minerals, and many others. While the initial stages of Lunar exploration will rely on transported equipment, long-term development – including construction, energy production, exploration, and valuable resource extraction – will depend on advancements in ISRU.

One of the most important resources available on the Moon is water-ice, most abundant at the South pole. The presence of and ability to mine ice on the Moon will be extremely beneficial for the development of a permanent Lunar presence. Water is of course crucial for life-support, as well as its constituent components hydrogen and oxygen. A wide range of studies have been conducted examining mining techniques [33] [34] [35], economic viability [36] [11], and Lunar ice characteristics and uses [37] [38] [39]. Lunar ice, while found in and around regolith, is not a component of regolith. Chapter 2 discusses the constituent elements of regolith, what can be extracted from regolith, and their uses and applications.

1.6. Research Objectives

The focus of this research is on the advancement of Lunar regolith brick production for Lunar and extraterrestrial development. A wide body of research has been conducted on different methods of sintering, casting, melting, and producing composites and concretes from Lunar regolith. While many experiments have proven the feasibility of producing bricks and other construction materials from regolith, a gap remains in the ability to manufacture usable, practically-sized bricks and construction materials. This research aims at reproducing and comparing two promising regolith sintering methods and analyzing their efficacy for usable brick production.

The first objective of this research is to define the criteria of usability so that each method can be fairly assessed across standardized categories. The literature will be referenced to

determine the most common assessments relating to construction-grade bricks. Construction applications with the highest demand will guide the selection of the most important parameters. A numerical score can then be assigned to the bricks taking into consideration each of the assessment categories. The methods will be analyzed for their general usability and potential for large scale production. Definitions, descriptions, and proposed grading schemes are included in Chapter 5.

The second objective is to produce Lunar simulant brick samples from promising sintering methods as discussed in Chapter 4. The data measured from these samples will serve as a contribution to the existing body of sintered regolith data and as a demonstration of the usability criteria as an analysis and comparison tool. The third objective involves assessing the samples under the usability parameters to determine each method's efficacy for producing construction-grade bricks for Lunar applications, which is discussed in Chapter 5.

CHAPTER 2

LUNAR REGOLITH FOR CONSTRUCTION

2.1. Lunar Regolith

The surface of the Moon is generally divided into two types of regions called Highlands; the higher altitude, older, and lighter-colored regions known for its highly anorthositic rocks and cratered appearance; and the darker Mare regions, which were formed by rapidly-cooling basaltic lava [40]. Ranging from a few meters to tens of meters thick, Lunar regolith is the result of hundreds of millions of years of meteorite impact on the Lunar surface which has pulverized the underlying bedrock into a fine gray powder. The soil contains agglutinates of lithic, mineral, and glass particles containing metallic iron which has been welded together by micrometeorite impacts [41]. Particle size distribution is known to be dependent on maturity (surface exposure time) and depth. This becomes important when considering that strength characteristics are dependent on grain size distribution [42]. Space-weathering is another environment-altering process involving the bombardment of low-mass solar-wind ions such as hydrogen and helium, and heavy ion exposure from solar flares and cosmic rays. These processes were reported on for their involvement in the formation of various rim types on Lunar soil grains [43]. High quality modal and chemical data was diligently documented by the Lunar Soils Characterization Consortium (LSCC) using scanning electron microscopy. Later, a broader range of data was

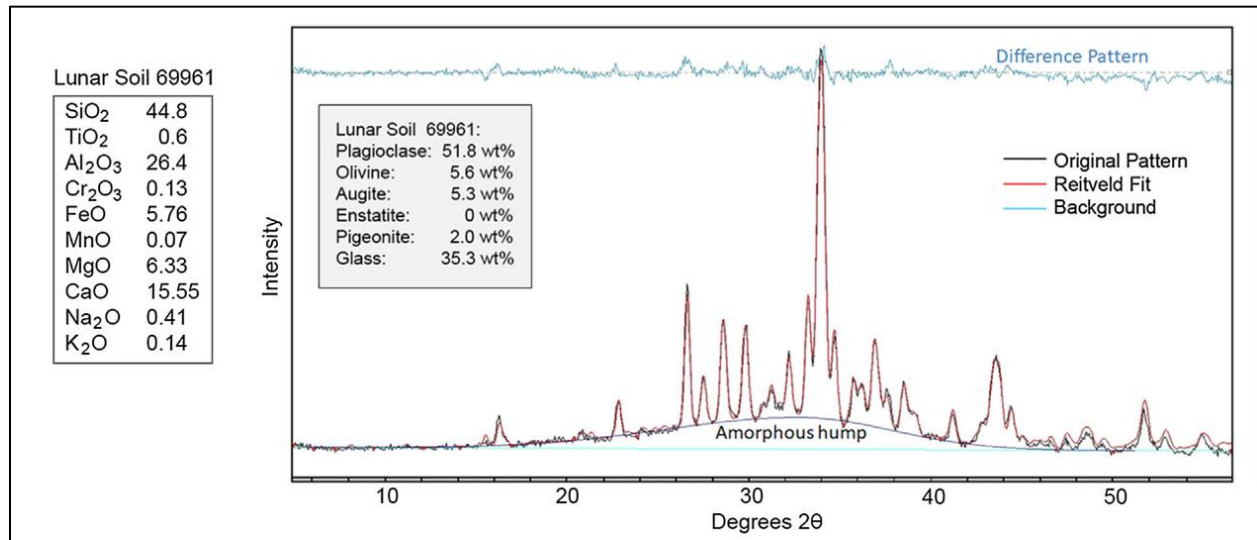


Figure 3. Example of Lunar regolith mineral composition from X-ray diffraction [44]

gathered using X-ray diffraction analysis on 118 Apollo soil samples, an example of which is shown in Figure 3, to determine precise mineral compositions [44]. The bulk percentage of Lunar soil is composed of silicon dioxide (approximately 45%), followed by aluminum oxide and calcium oxide (approximately 26% and 16%, respectively).

2.2. Regolith Simulants

Across six Apollo missions, 382 kilograms of Lunar samples were returned to Earth [45]. Soviet missions returned approximately 300 grams of regolith, and recent Chinese missions have returned another 2 kg [46]. Requests can be submitted to obtain Lunar samples from NASA, however, far more research is currently underway than can be supported by real Lunar samples. This introduces the need for simulant Lunar regolith that can be produced in large quantities and tailored to specific research needs. A NASA investigation in the early 1970's helped trigger the development of Lunar regolith simulants.

In 2006, NASA released a report entitled “Lunar Regolith Simulant Material: Recommendation for Standardization, Production, and Usage” for guiding the development of new simulants [47]. A 2021 paper by Toklu et al. provides an overview of each of the 54 existing simulants and the original studies citing their uses [46]. Each simulant has slightly different characteristics, whether it be mimicking different regions of the Moon, more accurate concentrations of titanium or minerals such as ilmenite, or a unique grain size distribution. In 1994, NASA developed a now popular Lunar regolith simulant called JSC-1 [48] to meet the demands of the growing scientific and engineering interest in lunar regolith experimentation. It is derived from volcanic ash from the San Francisco volcano field in Arizona, and it was designed to simulate Lunar mare regions for general use. LAO-1 is a Chinese regolith simulant designed to specifically replicate the characteristics of Apollo 16 samples. A significant portion of the research involving Lunar regolith doesn’t require authentic chemical or mineralogical profiles, such as research on rover wheel traction or excavation techniques. Low-fidelity analogue simulants, such as UoM-B and UoM-W presented and investigated by Just et al., are cheaper and more readily available for large-scale research projects [49]. Several additional simulant reviews have been published in recent years [50] [51] [52]. LHS-1 (Lunar Highlands Simulant), developed by Exolith Labs, was used in this research for its accurate representation of mineral and particle distribution of samples collected by the Apollo missions [53]. While LHS-1 may not be optimal for chemical processing, its accurate texture characteristics of polymineralic grains make it ideal for sintering and mechanical processing.

2.3. Uses of Lunar Regolith

Apart from solar power and the existence of water ice deposits, Lunar regolith is the only resource available on the Lunar surface. Fortunately, Lunar regolith is rich in useful elements such as oxygen, aluminum, iron, and titanium. It is abundant and easy to source [54] [55], it can be reacted with hydrogen to produce water and oxygen for life support and fuel [22], and when sintered (heated to just below melting temperature) can be formed into bricks for structures such as habitats and landing pads [56] [57] [58] [59] [10] [60] [61] [62]. Many studies have been conducted investigating the various applications of Lunar regolith and its constituent elements.

Among the most important resources for Lunar expeditions are water and oxygen. Evidence for water ice has been discovered in recent years at the Lunar south pole; the target landing site for Artemis 3 [63]. Oxygen, apart from being an essential element of life-support, is also a primary component of rocket fuels. Oxygen is present in a number of the minerals found in regolith, such as ilmenite. Hydrogen reduction of ilmenite produces water vapor. Electrolysis of the water yields elemental hydrogen, which can be recycled, and oxygen [22]. Other methods of oxygen extraction from regolith have been studied including mechanically-activated carbothermic reduction [64] and electrolysis of molten regolith [65]. Bennet et al. determined by optimizing non-linear scaling laws of system components that hydrogen and oxygen-based propellant sourced on the Moon can be more cost effective than transportation from Earth [11]. Regolith samples from the recent Chang'e-5 mission were studied by Yao et al. for their ability to operate as a catalyst converting CO₂ and water into elemental oxygen and hydrogen, methane, and methanol. This represents an important step in furthering the understanding of extraterrestrial photosynthesis technology and the production of Lunar fuels [66].

The extraction of volatiles and other elements from regolith has been explored. Thermal mining has been successfully tested as a means of extracting water and other compounds such as carbon dioxide and hydrogen sulfide from regolith simulants [33] [54]. A study by Volger et al. tested the feasibility of iron extraction from Lunar and Martian soils using microorganisms [67]. Volger describes these microorganisms, in this application, as “self-reproducing modifiable nano-factories, catalyzing a wide range of chemical conversions”. A paper by Guerrero-Gonzalez et al. compares three Lunar production plants for producing low-carbon steel, ferrosilicon alloys, and aluminum-silicon alloys from regolith [68]. The study concludes that scaling these facilities would increase production efficiency. Others have investigated the uses of these extracted materials. Stoll et al. introduced the concept of combining traditional manufacturing methods with 3D printing technology to produce rocket components from lunar regolith [10]. The paper considers the extraction of oxygen and aluminum from regolith for propellant and alloys for rocket tanks and fairings.

The properties of regolith lend themselves to a number of other useful applications. Regolith was considered for its heat storage capacities in a study about Lunar electricity production and storage. Raw regolith could be used to store heat surrounding a heat exchanger, and the author notes that sintered regolith would maintain the advantages of raw regolith while enhancing the thermal properties [4]. Furthermore, molten regolith was noted for potential latent heat storage. Among the greatest threats to human survival on the moon is the constant bombardment of radiation and the intense temperature variation, which regolith has been shown to defend against. The neutron radiation shielding properties of regolith were tested and determined to be similar to aluminum, with of course the added benefit of being sourced in situ [61]. Considering the extreme temperatures of the moon, Palos et al. describes the insulating

properties of regolith and states, "...a few tens of centimeters of lunar regolith could effectively isolate humans and equipment from the temperature variations above" [4]. These findings are crucial in planning the development of safe Lunar structures, especially for habitation and long-term human presence.

2.4. Regolith Sintering



Figure 4. In-house sintered Lunar brick sample (LHS-1 simulant)

Sintering is a process most often associated with the production of ceramics. It is a heat treatment process that bonds particles through mass transport at the atomic level. The bonded material experiences a significant increase in strength and decrease in surface energy. Melting,

on the other hand, involves the complete phase change of the material from solid to liquid. While it is true that sintering causes melting between grain boundaries, the material does not achieve a fully liquid phase. Sintering is a preferential process for application on the Moon due to its efficiency, considering that sintering occurs at just 50 – 70% of the melting temperature [69]. Sintering Lunar regolith produces a material analogous to concrete, evident in Figure 4. The first study involving the sintering of a Lunar regolith simulant was conducted in 1973 by Simonds [70] who was exploring the formation of Lunar breccia. Dozens of further studies have been conducted investigating different aspects of sintering Lunar regolith, such as the effects of particle size distribution [69] [71], temperature profile and heating and cooling rates [72] [73], mineralogy and glass content [74], and density [75], among others.

Porosity, which is determined by particle size distribution, is known to have one of the biggest influences on the strength of sintered regolith. Indyk et al. measured the mean compressive strengths of both low (1.44%) and high (11.78%) porosity sintered samples which were found to be 197.8 MPa and 71.3 MPa, respectively [69]. Gualtieri also confirmed that the increased packing density of fine regolith particles results in improved strength of sintered material [71]. Although its various components represent a wide range of melting temperatures, 1100°C is generally regarded as the target sintering temperature of Lunar regolith. Maximum temperature dictates the degree to which regolith grains melt which results in different textures and strengths. Furthermore, the heating rate and, more importantly, cooling rate of the sintering process determines strength performance via the mitigation of thermal cracking [73]. Mineralogy and glass contents vary among Lunar regolith and simulants. The presence of a glass phase (often omitted from regolith simulants depending on their use) has been shown to sinter more uniformly and at lower temperatures than fully crystalline regolith [74]. The following sections

describe the current state of some of the most prominent sintering methods for Lunar regolith at laboratory scale.

2.4.1. Furnace Sintering

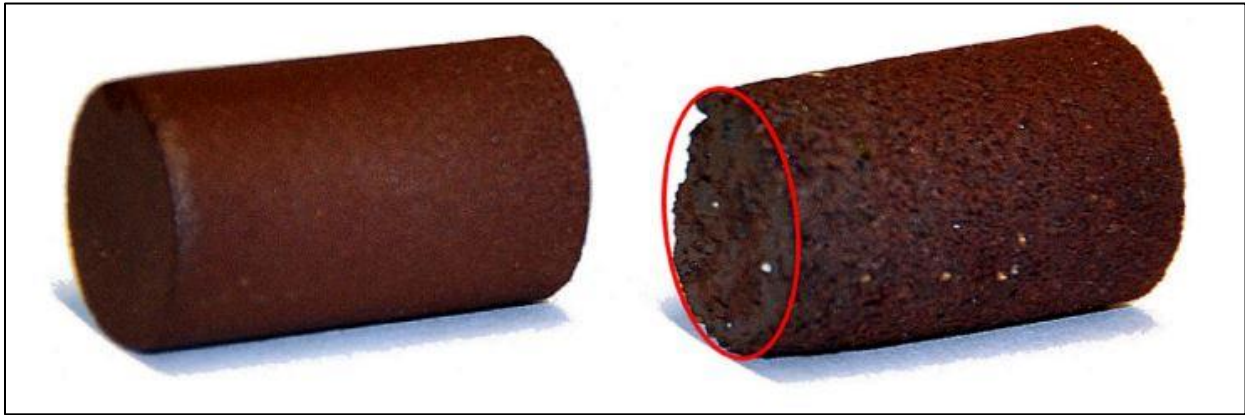


Figure 5. Furnace-sintered cylindrical bricks [69]

Furnace sintering is the simplest method for producing Lunar brick samples. Regolith is either poured into a high-temperature mold or cold-pressed into a green body [69] before being placed in a furnace. Hot-pressing involves applying continuous pressure during the heating period which improves particle contact [70]. Sintering in a furnace allows precise control over the heating regime. A simple controller is usually sufficient to select an appropriate heating and cooling rate, maximum temperature, and hold duration. Laboratory furnaces also provide the option for sintering in unique atmospheres such as nitrogen or argon. This makes it the preferred method for studies investigating the impact of varying sintering parameters within a controlled environment.

A paper by Farries et al. provides comprehensive overviews of various regolith sintering methods including 14 furnace sintering studies [75]. There is a wide variety of sintering parameters used, including varying simulant types, grain distribution, heating profile, cold-press

pressure, atmosphere type, and resulting dimensions, density, and compressive strength. Eleven studies reported maximum sample dimensions, which ranged from 19.1 mm to 180 mm. Most notable are the compressive strength results, which were reported by only seven of the studies, five of which reported ranges of produced strengths. Across the seven studies, the strength ranged from just 2.8 MPa up to 232 MPa. Three of the seven studies managed to produce at least some samples above 200 MPa [69] [71] [76]. Considering that terrestrial concrete typically displays compressive strengths of about 17 – 28 MPa [77], radiant furnace sintering of Lunar regolith has significant potential in producing high strength material.

2.4.2. Concentrated Solar Sintering

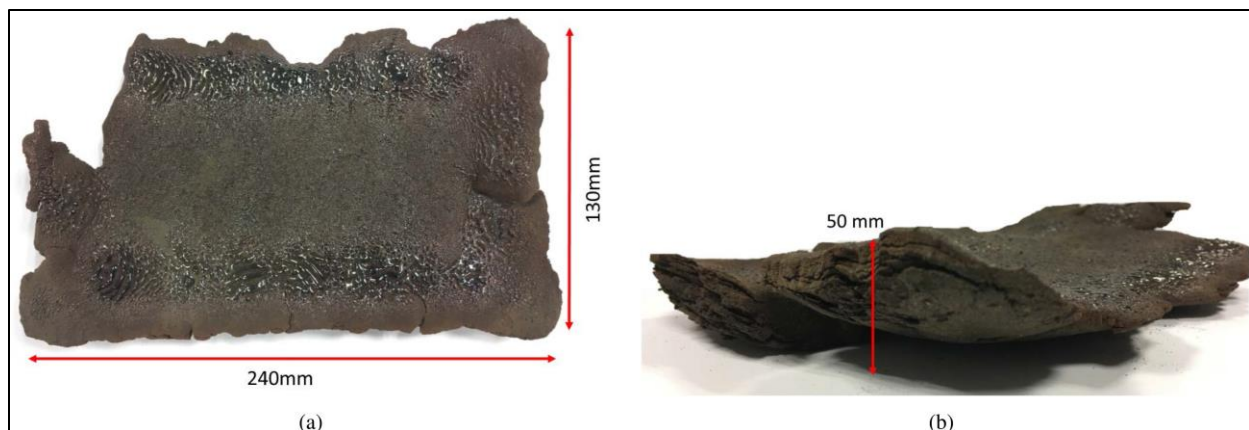


Figure 6. Regolith simulant slabs sintered with concentrated solar light [85]

Considering that the only directly available energy source on the Moon is sunlight, the use of concentrated solar energy has been of interest for sintering Lunar regolith. The first study involving this direct sintering approach was conducted by Cardiff et al. in the development of a dust mitigation vehicle for the Lunar surface [78]. A high-vacuum chamber was constructed around a crucible of regolith simulant and a lens-equipped remote-controlled vehicle focused solar light on the sample. Surface sintering rates as high as 13 cm²/min were achieved. A similar

study for stabilizing surface regolith was conducted by Hintze et al. using a mobile Fresnel lens [79]. Hintze was able to achieve sintering depths of 6 mm when the lens was held stationary and just 1-2mm when moved across the surface. Notable problems shown with concentrated solar sintering include first the depth of penetration, which is insufficient in a single pass to produce a hard, stabilized layer, and second the tendency of the regolith to densify and crack under the high thermal gradient caused by the small light incident. Surface cracking is especially prevalent with an uneven surface which would be considerable on the Moon. Compacting the regolith before sintering would likely reduce densification during heating and even the surface for a smoother finish, but this of course adds another level of complexity to the process. Limited material properties exist for sintered samples via concentrated solar, but Hintze reports penetrometer strength of 0.6 MPa of the stabilized surface material [79].

2.4.3. Microwave Sintering



Figure 7. Microwave-sintered samples of regolith simulant [114]

While radiant heating and concentrated solar both rely on heating regolith from the outside in, microwave sintering has been proposed, in some cases as a supplement to radiant heating to evenly heat the material from the inside. Microwave radiation is the range of electromagnetic frequencies between 300 MHz and 300 GHz. Due to the nanophase FeO

abundant within the silicate glass in Lunar regolith which helps reflect radiation, it is considered extremely coupled to microwave radiation. Therefore, regolith can be completely melted in a conventional 2.45 GHz microwave oven in a matter of minutes [80]. Thermal runaway is a challenge associated with microwave heating, in which the energy is absorbed at a higher rate by the center of the material and the outer surfaces remain less affected. This phenomenon has led to the proposal of hybrid heating schemes, where the hypothetical superposition of microwave and radiant heating could more evenly heat a sample [81]. Even heating generates a lower thermal gradient which theoretically would reduce heating and cooling microfractures that tend to decrease the material's strength.

Farries et al. also summarizes the parameters and outcomes of previous microwave sintering trials [75]. Notable results from these experiments by other researchers include maximum sample dimensions ranging from 10 mm to 40 mm across hybrid and pure-microwave trials. No strength data was reported for pure-microwave sintering, but hybrid experiments yielded compressive strengths between 0.4-26 MPa. A study by Gholami et al. produced hybrid-microwave samples with compressive strengths of 45 MPa [82]. While the upper end of this data is promising compared with the strength of terrestrial concrete, the strengths reported from furnace-sintered samples still far exceeds these hybrid experiments. Farries concludes, "For sintering, efficiency gains from rapid microwave heating are irrelevant because of the low heating and cooling rates needed to avoid high thermal stresses and cracking. While further data are needed on the energy efficiency of all potential processes, it is likely that microwave sintering will be less efficient and have lower production rates than radiant furnace sintering or casting..." [75]. Further studies in microwave sintering should be studied to determine if efficiency and production rate can be improved.

2.4.4. Additive Manufacturing

Additive manufacturing, also known as 3D printing, has surged in popularity as an extremely flexible fabrication technique. Typically, three-dimensional objects are created from a solid computer model by consecutively depositing many thin layers on top of one another. Several methods of additive manufacturing for producing lunar bricks have been tested. Altun et al. mixed finely sieved regolith simulant suspended in a photocurable ceramic binder. Using a commercially available ceramic 3D printer, researchers were able to print and sinter miniature structures on the order of about 1 cm, which included nozzles, gears, screws, and even a model of St. Stephen's Cathedral, with remarkable precision [59]. Physical Science Inc. developed a system that uses solar concentrators and a fiber optic cable to direct solar radiation to a movable head [83]. Large 15 x 15 in. pads were sintered. Due to the large focal point the printing resolution was low, and no mechanical property data was recorded. NASA's Jet Propulsion Lab proposed a lunar rover-based system utilizing similar optic cable technology. Equipped with an onboard solar concentrator and freeform additive manufacturing arm, the design would allow for mobile construction [84]. This would likely be useful for large surface area construction such as landing pads and roads. Meurisse et al. developed a layer-by-layer 3D printing method for sintering lunar regolith using an array of xenon arc lamps [85]. By translating a bed of regolith simulant beneath the beam of solar radiation, an area of approximately 120 mm by 240 mm was able to be sintered. After each surface irradiation, 0.1 mm layers of unrefined regolith were applied, resulting in a maximum thickness of 50 mm in some locations. The team was able to produce brick-shaped samples in about 5 hours. While the specimens were significantly larger than what has been produced previously, compression testing of the samples yielded poor results of approximately 2.3 MPa. The team designed follow-up experiments to confirm that stronger

specimens could be produced by reducing the cool-down time between layers. This was achieved by reducing the sintering surface area thereby reducing time between layers. This research made progress into increasing the size of sintered lunar bricks by physically moving the bed of regolith to irradiate a larger area. Still, the bricks produced in this study would not satisfy strength or uniformity characteristics required in construction applications. Further work is needed to improve large scale lunar bricks.

CHAPTER 3

USABILITY CRITERIA

3.1. Usability Criteria Overview

Regarding sintered regolith bricks, there are a variety of important parameters to be considered that would qualify a brick (or sintering method) to be useful for Lunar construction. For safety and durability, certain material property standards must be met. A range of brick sizes and shapes will be necessary, most of which are much larger than the samples presented in the relevant literature. Finally, various efficiency-based parameters such as the energy cost per volume of sintered regolith and required infrastructure for manufacturing must be analyzed. Each criterion is weighted according to its relative importance on a 1-5 scale shown in Table 1. Within each criterion, four levels have been determined which a brick or sintering method can be assigned (4 is the highest score). Four grading levels allow a certain confidence in the differentiation and consistency across the criteria. A grading scheme with fewer levels was found to be too coarse, and grade levels beyond four became arbitrary and reduced the certainty of differentiation. This section proposes, examines, and ranks the various usability parameters relevant to sintered regolith bricks listed in Table 2.

Previous sections explored the history of Lunar research and development, some of the goals for future Lunar missions, and the current state of sintering methods and technology in support of these goals. The Usability Criteria targets the next phase of Lunar development involving ISRU and the first structures for permanent human presence. The context for this evaluation tool is regolith sintering methods and the capacity for less than a dozen Lunar inhabitants.

Table 1. Usability Criteria importance factors and descriptions

Importance Factor	Description
5	<ul style="list-style-type: none"> • Critical, highest priority, primary focus • Stringent, low flexibility
4	<ul style="list-style-type: none"> • Essential, high priority, key element • Few valid approaches or solutions
3	<ul style="list-style-type: none"> • Important, significant • Several possible approaches or solutions
2	<ul style="list-style-type: none"> • Considerable • Wide range of approaches or solutions
1	<ul style="list-style-type: none"> • Worthy of consideration, low priority

Table 2. List of Usability Criteria with weights

Criterion	Weight
Energy Cost per Unit Volume	5
Compressive Strength	4
System Versatility	4
Production Rate and Mass Efficiency	4
Labor Requirement	3
Uniformity	2
Hardness	1

3.2. Compressive Strength (4)

Maximum compressive strength is a measure of a material's capacity to resist the pressure caused by a compressive force. This makes it the most practical mechanical property of interest regarding Lunar regolith considering that many of its applications are in load bearing structures. Framed structures, such as wood or steel-framed buildings built on Earth, rely heavily

on tension as well as compression to manage loads. Brick and stone structures, however, including brick houses, archways, and walls, depend on the combined compressive strength of each block to bear the structure. Toklu et al. writes, “Especially the compressive strength value of construction materials is conventionally used in the field of civil engineering in order to define the quality and the performance grade of the materials of concern” [46]. While advanced building techniques and clever geometry can be used to maximize a structure’s integrity, an understanding of the basic strength of each individual brick is a principal component in the design process.

The procedure for strength testing of sintered regolith in the relevant literature is consistent with methods used for other materials such as composites and concretes. This procedure typically involves the production of uniform sintered specimens, often cylindrical in shape, followed by compression testing with a load cell [69] [71] [86] [87]. Gualtieri et al. compacted regolith simulants into cylindrical dies with approximate height to width ratios of 2:1 prior to sintering. A universal compressive test machine was driven at 0.5 mm per minute until fracture [71]. For compression testing large sheets of sintered material, 20 mm cubes were cut from the sheets, and the top and bottom surfaces were coated with concrete to create flat planes [85]. Several studies have also investigated flexural strength of sintered lunar specimens using traditional three-point bending systems [87] [60]. While compressive strength is by far the dominant material property of interest for sintered regolith, flexural strength may be determined to be an important addition in the future. Both cylindrical and prismatic lunar regolith samples have been used in flexural tests. A wide range of maximum compressive strengths have been produced from sintered regolith (simulant) samples, from 2 to well over 200 MPa. High-strength concrete rarely exceeds 70 MPa, with most applications requiring between 17 and 28 MPa.

The standards for compressive strength of terrestrial construction-grade bricks vary. The American Society for Testing and Materials (ASTM) Code 67 for minimum strength of building bricks requires from 8.6 to 17.2 MPa depending on brick grade [88]. The Indian Standard (IS 1077:1992) classifies bricks ranging from 3.5 to 35 MPa. Building Design Standards (BDS) have a minimum strength range of 10.3 to 24 MPa [89]. To translate these standards to the lunar environment, it should first be noted that the gravitational pull on the lunar surface is $1/6^{\text{th}}$ that of Earth's. This means that the mass of a structure on Earth would exert $1/6^{\text{th}}$ the downward force on the Moon [32]. In other words, materials would have six times the load bearing capacity on the Moon than on Earth. This suggests, considering terrestrial brick standards and the relative strength of materials on the Lunar surface, that strengths of sintered Lunar brick samples already produced would far exceed the strength performance of standard construction bricks on Earth. Farries states that "... on the Moon, where establishing processing equipment is extremely expensive, the material savings that can be made by employing high-strength materials are critical" [75]. Durability and safety are of maximal importance on the moon, however, and a Lunar factor of safety would need to be significantly higher than that on Earth. This is to say that sintered Lunar regolith exhibits promising strength characteristics for simultaneously achieving high factors of safety while minimizing material requirements.

Conducting compressive strength tests yields basic force (N) vs deflection (mm) data. Some analysis of the force-deflection curve must be done to determine if local failures have occurred before ultimate failure of the specimen. Ultimate strength can be determined by dividing the maximum experienced force before ultimate failure by the specimen's cross-sectional area.

A logarithmic curve was fitted between a practical minimum of 2 MPa and a maximum cutoff of 300 MPa, beyond which no results have been demonstrated. This allows a large range of values that are roughly the strength of terrestrial concrete and higher to be graded a 3 or 4. If Lunar regolith is sintered effectively, it will almost always achieve this strength grade. Methods that do not achieve at least 10 MPa likely need significant refinement to be considered a structural material. Strength parameter details are shown in Table 3.

Table 3. Compressive strength grading parameters

Grade	Compressive Strength	As Strong As	Usability
1	< 2 MPa	- Balsa - Rigid foams - Cork	Poor structural material
2	2-10 MPa	- Silicone - PVC	Some structural applications
3	10-50 MPa	- Structural concrete - Laminates - Lead	Sufficient for most Lunar applications
4	50-300 MPa	- Porous ceramics - Glass - Zinc alloys	Suitable for high-strength applications

3.3. Hardness (1)

Hardness is the ability of a material to resist localized plastic deformation including scratching, penetration, and indentation. Ceramics, such as silicon-carbide, are well known for their remarkably high hardness and other properties such as an extremely high melting temperature. Hardness is not a fundamental material property and is usually evaluated in consideration with other properties such as strength and ductility, but it plays an important role in material engineering. Hardness, measured by Rockwell testing, was determined to be a reliable

method for determining compressive strength of polymer concrete based on a linear relationship between the two properties [90]. Materials with high hardness typically display a high resistance to impact and wear, however, they also tend to be highly brittle and therefore do not lend themselves to structural applications.

Concerning Lunar construction, producing sintered material with high hardness may not be beneficial where strength is concerned, but in applications where resistance to impact and other types of wear is crucial. High hardness may be essential in structures for protection from meteorites, on roads for durability, and in barriers for shielding against rocket plume ejecta. Despite these important applications, a significant gap exists in the relevant research concerning this material property. Very few studies involving sintered Lunar regolith measure or report hardness. Gholami et al. studied the microstructure and mechanical properties of hybrid-microwave-sintered regolith simulant including nano-indentation hardness, but little discussion is had about its importance [82]. Due to the lack of existing hardness data in the literature, no evaluation parameters are set forth. A better understanding of the hardness properties of sintered regolith may expand its potential uses and influence the selection of sintering methods on the Moon.

3.4. System Versatility (4)



Figure 8. ESA's hollow closed-cell concrete structure 3D-printed simulating regolith characteristics [91]

The different sizes, shapes, and intended uses of structures built on the Moon will necessitate a certain diversity in brick types. Figure 5 shows a large block of a 3D-printed structure using regolith-simulating concrete produced by the European Space Agency [91]. Several habitat designs have been proposed with different solutions to the myriad challenges of Lunar construction including structural integrity, temperature fluctuation, and air pressure. A universal brick-and-mortar construction style will not be sufficient for the Lunar environment. For casting bricks from molten regolith, it is understood that a variety of molds would be required to produce bricks of different sizes and shapes, and the same is true for sintering methods. Zhou et al. proposed and analyzed an automated robotic system for construction of a modular hangar-style structure composed of prefabricated, 3D printed blocks [56]. Including interlocking rectangular blocks and arched segments, a total of four unique and relatively complex block shapes were proposed in the design. In a separate publication by Zhou et al, a

Deep Convolution Neural Network was used to identify six brick shapes for use in assembling various styles of structures [57]. Again, 3D printing was proposed for the fabrication of the unique brick shapes. As discussed previously, other Lunar architecture is necessary apart from buildings including landing pads, roads, bridges, and berms. While it may be possible in the far future to have differentiated sintering units (e.g. a rover for sintering roads, a 3D printer for buildings, a truss fabricator for bridges, etc.) the early stages of Lunar development must rely on versatile equipment due to mass limitations.

While the concept of “versatility” isn’t explicitly explored in the relevant literature, work has been done to advance the technology regarding manufacturing modularity. This is especially evident within the field of additive manufacturing with proposals such as a novel cable-driven printing architecture [92] and a movable fiber optic cable head for directing solar energy [58]. Altun et al.’s experiments with ceramic-regolith mixtures displayed a remarkable ability to print miniature objects with high precision, using radiative heating to sinter them post-fabrication [59]. Of course, to print the blocks proposed by Zhou et al.’s work which are on the order of 1 meter, ceramic-printing technology would need to be scaled up significantly. The versatility of additive manufacturing is inherently far greater than other methods such as radiative or microwave sintering due to the fact that this technology was specifically developed for versatile fabrication. The four grade levels of system versatility are shown below, with examples from the literature included.

1. No Versatility

Literature Examples: [69] [79]

- a.** Single output capacity
- b.** Invariable dimensions
- c.** Incapable of equipment interchange or requires significant adjustment

2. Low Versatility

Literature Examples: [58] [85] [75] [82] [59]

- a.** Capable of limited versatility
- b.** Single adjustable dimension
 - i. (e.g. small, detailed shapes or large, simple shapes, but not both)

3. Moderate Versatility

Literature Examples: [93]

- a.** Multiple outputs
- b.** Capable of full-structure fabrication

4. High Versatility

Literature Examples: [92] [91]

- a.** Wide variety of output types
- b.** Capable of full-structure fabrication
- c.** Capable of multi-structure fabrication (habitat, bridge, etc.)
- d.** Zero/minimal equipment interchanging/adjustment

3.5. Energy Cost per Unit Volume (5)

During initial Lunar development energy will be a scarce resource, and the energy efficiency of all Lunar systems will be heavily scrutinized. While some construction methods can bypass a significant energy demand, such as additive manufacturing with regolith cements, this work considers only methods that produce sintered regolith material. The literature regarding sintered regolith varies in its reporting of energy usage or efficiency. Isachenkov et al. thoroughly evaluates the results of 10 additive manufacturing methods including a summary of energy usage [58]. On the other hand, as Farries concludes, “The data from experimental trials of direct solar and radiant heating is insufficient to accurately estimate sintering rates and embodied

energy” [75]. A clear consensus has not yet been reached on standard or acceptable energy efficiency.

Production of power on the Lunar surface is a central challenge in regard to establishing a Lunar base. The most prominent contenders for electrical power include photovoltaic (PV) cells, nuclear fusion or fission, and Lunar hydrogen and oxygen fuel cells [6]. Photovoltaic cells have a significant advantage due to being lightweight, modular, and reliable. While their primary drawback is being only operational during “daytime”, there are locations on the Lunar surface where sunlight is constant. Nuclear power provides constant power and has a better power-to-mass ratio than PV. NASA expects to employ PV cells during initial development with the integration of a nuclear reactor later [94] [23]. However, if a requirement greater than 100 kWe is estimated for initial development, PV may be skipped except as an emergency power source. The minimum for human power consumption has been estimated to be at least 3 kWe per person. For ISRU, the power consumption of mining and processing equipment is estimated by NASA to be between 500 and 1000 kWe to start [94]. Palos et al. suggests a similar multi-stage power generation plan with 25 kWe to start ramping up to 180 kWe for ISRU development [4].

Currently, power requirements or embodied energy of sintering methods is not a significant component of research results despite being an important consideration for the Lunar application. The methods that most often report energy data are microwave and selective laser sintering due to the easily available power information associated with them. A simple calculation involving the power consumption (accounting for losses) and volume rate of sintering can provide a normalized unit of kJ/cm^3 for comparison between different studies and methods. Only rough estimates exist for cast or radiant heating methods [95] such as comparison with clay brick production [96]. Nakamura et al. estimated the solar power entering the fiber optic cable of

their system at 540 W, but without a reported sintering volume rate it is difficult to compare. Optimistic estimates of radiant sintering yield the most efficient energy usages of less than 5 kJ/cm³. Hybrid microwave and selective laser sintering experiments occupy the mid-range. A method called Laser Engineered Net Shaping (LENS), involving the deposition of regolith powder in an inert gas flow and melting with a laser (analogous to MIG welding), was found to use energy an order of magnitude higher than even low-efficiency laser sintering methods [97]. Greater emphasis on the energy efficiency of sintering methods is needed in future research.

A logarithmic curve was fitted between a theoretical minimum of 0 kJ/cm³ and a maximum cutoff of 150 kJ/cm³, beyond which only extreme outliers fall. This weighted curve allows for a thin margin of energy usages to be given a top grade, with increasing bin ranges as energy consumption increases. Specific energy parameters are shown in Table 4.

Table 4. Energy requirement grading parameters

Grade	Normalized Energy Requirement	Results from Previous Studies
0	>150 kJ/cm ³	8.3 MJ/cm ³ [97]
1	50-150 kJ/cm ³	135.7 kJ/cm ³ [82] 90 kJ/cm ³ [98]
2	25-50 kJ/cm ³	31.2 kJ/cm ³ [99]
3	10-25 kJ/cm ³	16.9 kJ/cm ³ [100] 11.23 kJ/cm ³ [84]
4	< 10 kJ/cm ³	9.75 kJ/cm ³ [101] 3.9 kJ/cm ³ [102] 1.94-2.47 kJ/cm ³ [103] 1.87 kJ/cm ³ [104]

3.6. Labor Requirement (3)



Figure 9. Artistic rendition of ICON's Lunar additive manufacturing technology [105]

Especially for the earliest Lunar return missions, but in general, the activity of astronauts on the Lunar surface will be a carefully balanced and largely choreographed operation. The strict limit of resources and life-support systems will necessitate an optimized schedule for all personnel. While the establishment of a permanent base will afford astronauts a higher level of security and freedom, they will still ultimately be ‘on the job’. Kathy Lueders, associate administrator for human spaceflight at NASA Headquarters in Washington, said, “On each new trip, astronauts are going to have an increasing level of comfort with the capabilities to explore and study more of the Moon than ever before” [23]. Artemis 3 will land two astronauts on the Lunar South Pole – chosen for its potential access to water ice and other mineral resources – where their primary objectives will be to explore and conduct science. Studying this region and confirming the presence of these resources is an incredibly important step for the future of Lunar development. Every minute that astronauts must spend tending to equipment and systems that

could theoretically be automated detracts from their primary objectives and reduces the value of the mission.

This idea of time efficiency is and will be an important consideration for regolith sintering and construction. At the laboratory scale, where most sintering methods currently exist, there is a range of operation and attention requirements. For example, direct sintering with concentrated solar light requires manual focus and beam maneuvering, whereas radiant or microwave heating can be left unattended for the sintering duration. At full-scale, sintering equipment will still have a range of automation, and those that require the least amount of astronaut involvement will be preferential. Fully automated additive manufacturing is already being selected as the frontrunner technology. In November of 2022, NASA awarded a contract to a private company called ICON, which specializes in 3D printed homes, to develop this technology for construction on the Moon [105]. A rendering of this technology is shown in Figure 9.

1. High Labor

- a. Manually operated (i.e. excavation, filling molds, operating robotics)
- b. Requires operator(s) for initialization
- c. Major intervention/reset between assignments

2. Moderate Labor

- a. Requires consistent monitoring
- b. Some initialization before operation
- c. Major intervention/reset between assignments

3. Minimal Labor

- a. Requires minimal monitoring (i.e. visual check between AM layers)

- b. May require set-up before each assignment
- c. Simple reset between assignments

4. Fully Automated

- a. Autonomous
- b. Capable of full-scale construction
- c. Multiple assignments without operator intervention

3.7. Brick Uniformity (2)

In any manufacturing process the uniformity of the product must be examined. There is typically a small percentage of defects that are taken into consideration due to inconsistencies in the raw material or variations in the manufacturing process. In clay brick production, for example, there are a number of common defects that a certain percentage of bricks are expected to have such as air pockets, cracks, rounded corners from improper casting, efflorescence from the presence of alkalis, and over- or under-firing. Not all of these issues translate to the Lunar application, but understanding the issues present in terrestrial brick-making may be important in addressing the potential issues regarding Lunar bricks. Cracks due to water or voids, staining or mineral interference, and improper sintering level may result in defects in mass-production of sintered Lunar bricks.

It can reasonably be assumed that cast regolith (sintering in a mold) will produce more uniform bricks than sintering with direct solar energy. Furthermore, the material properties of a brick that was sintered with refined regolith are more likely to be consistent than bricks sintered with raw regolith. Lunar regolith varies from region to region and between samples from the same region, meaning the sintering or refining methods will need to be location specific. In most manufacturing systems, some percentage of units are extracted during production and tested to

ensure quality and consistency. It is suggested that for methods producing discrete units (bricks), among the parameters relating to uniformity should be measurements comparing sample dimensions, compressive strength, mass, degree of sintering, and surface smoothness. Non-discrete sintering methods, such as 3D printing, will require unique testing methods. One solution may be to print individual units for layer-width and compressive strength measurements, or a singular wall segment to test linear variations in quality.

Exact parameters for acceptable limits on sintered regolith defects and variations have not been established. The literature regarding sintering methods rarely addresses issues related to mass production of sintered material due to the fact that laboratory experiments typically deal with small sample sets. As large-scale prototypes are developed for Lunar brick production, a clearer definition of the parameters relating to brick quality will be required. Precise parameters, such as the acceptable error limits for brick dimensions or compressive strength, are not yet proposed. More information is needed, likely with input from institutions such as NASA, before a practical grading scheme can be created.

3.8. Production Rate and Mass Efficiency (4)

It has already been established that time is an extremely limited resource during Lunar missions and especially for earlier return missions. Assuming all necessary safety measures and standards are met, the total construction time for Lunar structures is another influential parameter in the method selection process. It can be assumed that the process of mining, refining, sintering, and constructing a lunar habitat will take a considerable amount of time with the limited infrastructure of early Lunar development. Habitat designs on the extreme ends of potential time frames are omitted from this evaluation. As discussed in section 1.4, it has been suggested to use

inflatable structures or to reuse rocket fairings and fuel tanks for rapid habitat deployment in just hours or days. At the other extreme are much larger permanent structures, such as the proposed 2000 square-meter Roman Pantheon-inspired habitat with an estimated build time of 3 years [106].

Standardized habitation design parameters are borrowed from Zhou et al. who presented an automated robotic assembly system for a habitat structure designed for 3-6 inhabitants with dimensions of 14m x 8m x 5.5m. The arched, hanger-like structure is composed of six different brick shapes totaling a volume of 141.62 cubic meters of sintered regolith. The authors assume a sintered density of 2500 kg/m³, which would result in total structure mass of 354,050 kg [56]. While this only accounts for a single structure (and other designs may require different amounts of sintered regolith), it is a reasonable value for comparison purposes.

In recent years, 3D-printed structures like the clay Tecla houses [107], can be printed in about 200 hours. While the size of these structures is similar in magnitude to proposed Lunar habitat designs, the amount of material required for safety, insulation, and radiation shielding on the Moon is far greater. The sintering rate for the production of Zhou et al.'s design in 200 hours would need to be 1,770.25 kg/hr or approximately 30,000 g/min (the units often represented in the relevant literature). Farries et al. provides a summary of regolith additive manufacturing techniques including results from eight studies that calculated sintering rate [75]. These values ranged from 0.1 to 10 g/min: at best 3 orders of magnitude shy of the 200-hour target.

Limited information is available on the expected or acceptable time frames for Lunar construction. A range of potential mass deposition rates can be estimated based on the state of the current additive manufacturing technology. Most large-scale extrusion printers have nozzle diameters of approximately 6 mm to 50 mm, and linear extrusion rates of 50 mm/s to 500 mm/s

[108]. Taking the largest nozzle size, the range of volume flow rates are approximately 98.1 cm³/s to 981 cm³/s. The cements used in these printers vary, but a reasonable density can be assumed to be 2 g/cm³ which is similar to Lunar regolith (LHS-1 simulant has a density of 1.3 g/cm³, and the sintered density assumed by Zhou et al. was 2.5 g/cm³). Estimated mass flow rates fall between 11,781 g/min to 117,810 g/min. When applied to the previously estimated Lunar habitat mass, the potential range of construction times falls between 50 and 500 hours. While these estimates are based on wet extrusion of cements (which relies on curing rather than sintering or melting), and the primary focus of this research is dry-sintered regolith, it is still a useful target as the apex of rapid construction technology. Additive manufacturing technology is growing exponentially as a rapid and inexpensive (terrestrial) construction technology but adapting the technology to the Lunar environment has only just begun. Improving the sintering approach, solving extrusion and equipment stability in low gravity, and equipment performance in the intense thermal gradient and vacuum are a few of the engineering challenges yet to be solved. The current body of sintered regolith research has had a primary focus on pioneering new methods and understanding the material characteristics of the samples produced, but little attention has been directed towards large-scale production of sintered regolith. This is an area that will require significant advancements before any method becomes capable of Lunar construction.

The concept of ISRU is central to the technologies of sintering and the commitment to producing structures from regolith. The push for ISRU, as discussed in Chapter 2, is due to mass launch limitations and the extreme cost of space transportation. Mass of equipment brought to the Moon is a significant portion of the total cost equation. If production speed was the most important factor, the size or number of construction units would simply be increased. While it is

certainly true that the amount of equipment will slowly increase into the future of Lunar development, the feasibility of early Lunar construction projects will rely on lightweight systems. Therefore, it is important that the output capabilities of production methods are balanced with total equipment mass.

A basic scale of equipment masses in three categories is proposed which, while they will likely be adjusted as Lunar construction technology improves, provides a starting point for evaluation. The Lunar Roving Vehicle (LRV), at 210 kg, is an example of lightweight equipment that has already been used on the Lunar surface. It can be assumed that sintering and construction equipment will be significantly more advanced and greater in mass than a simple rover. The original Lunar landing module weighed approximately 15,000 kg fully loaded. The dry masses of the ascent and descent stages of the module were approximately 2,445 kg and 2,034 kg, respectively. These may serve as reasonable “standard” masses for construction equipment. Another data point to consider is the estimated cargo mass of the Starship Human Landing System – already awarded a contract from NASA for the Artemis missions – which is reported to be over 90,000 kg (100 tons) [12]. Assuming that just over ten percent of the cargo mass is dedicated to construction equipment, a mass of 10,000 kg will serve as the upper limit for the heavyweight category. For further context, the estimated mass of sintering and construction equipment for the Lunar mega structure proposed by Woolf et al. was suggested to be 50 tons (50% of Starship’s capacity); an estimate well outside of the initial development stage figures [106].

The proposed grading scheme favors low mass systems, allowing the highest grade for lightweight systems at a wide range of sintering rates. In the future, it can be expected that it may be both possible and worthwhile to consider transporting equipment far outside the mass and

sintering rate categories discussed here. Systems of this scale would likely only make sense once the level of infrastructure that this evaluation is focused on has already been established. The proposed categories and limits offer a practical starting point for early-stage Lunar construction efficiency-analysis. Estimated production rate levels are shown in Table 5 along with build-time for the standard structure. This production rate can be combined with equipment mass shown in Table 6 to determine a final grade.

Table 5. Production rate levels

Production Level	Sintering Rate	Corresponding Build Time for Standard Structure (354,050 kg)
Fast	3,540 kg/hr	< 100 hours (~4 days)
Moderate	708-3540 kg/hr	100 – 500 hours
Slow	354-708 kg/hr	500 – 1000 hours
Gradual	<354 kg/hr	> 1000 hours (~41 days)

Table 6. Mass Efficiency grading parameters

Mass Level	Prod. Rate	Grade
Lightweight (<1000 kg)	Fast	4
	Moderate	
	Slow	
	Gradual	3
Fast		
Moderate		
Slow		
Standard (1000-10,000 kg)	Gradual	2
	Fast	
	Moderate	
	Slow	
Heavyweight (>10,000 kg)	Gradual	1
	Fast	
	Moderate	
	Slow	

CHAPTER 4

EXPERIMENTAL METHODS AND RESULTS

4.1. Methods

A primary objective of this research was to produce samples of sintered regolith bricks from established, promising sintering methods that can be used to apply the usability criteria to and to contribute to the existing body of sintered regolith brick data. The first method uses a high-temperature laboratory furnace to sinter regolith in a mold following a predetermined heating profile. The second method combines concentrated solar energy with a simplified additive manufacturing procedure to sinter bricks layer-by-layer. As discussed previously, furnace sintering and additive manufacturing are two sintering methods that have a significant amount of previous research support and are considered among the most promising sintering methods. The bricks produced from these two methods are distinct and will provide unique scoring across the usability criteria.

4.2. Lunar Highlands Simulant

The LHS-1 Lunar regolith simulant was used in all experiments. Apart from being inexpensive and widely available, LHS-1 was developed to mimic Lunar Highlands regolith which constitutes much of the Lunar South Pole: the target for the Artemis 3 base camp. Therefore, this type of regolith will likely serve as the raw material for the first Lunar sintering and construction projects, making it an appropriate simulant for sintering experiments. LHS-1 is composed of 74.4% anorthosite, 24.7% glass-rich basalt, 0.4% ilmenite, 0.3% pyroxene, and 0.2% olivine, by weight [53].

4.3. Furnace Sintering: Furnace Setup

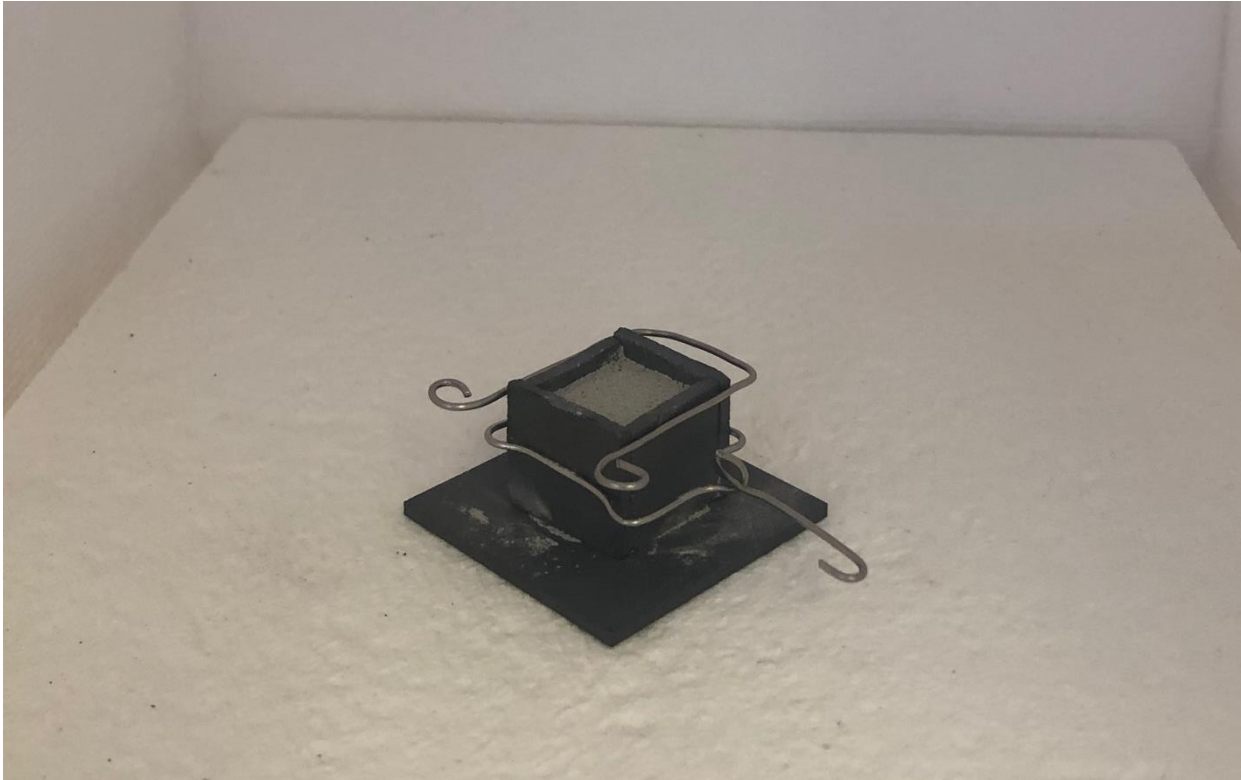


Figure 10. Silicon carbide mold containing regolith simulant

As discussed in section 2.4.1, various strategies are used in the literature for containing regolith samples for heating in a furnace. Due to the availability of thin, 1.5 in. x 1.5 in. silicon carbide plates, a simple mold was constructed (shown in Figure 10). One plate served as the bottom, upon which four walls were placed made each of one quarter of a second plate. The walls were secured together with handmade stainless-steel wire clips. The steel clips decayed in the furnace and were re-fashioned for each experiment. After approximately 10 experiments at high temperature, the silicon carbide surfaces became rough and began fusing to the regolith simulant and the mold itself was remade.

4.3.1. Furnace Sintering: Initial Trials



Figure 11. Lightly-sintered test sample

Several different high-temperature laboratory furnaces were tested and used to sinter samples. A total of seven samples were sintered using two different furnaces each with maximum temperatures of 1100°C. A range of sintering times were tested to determine adequate sintering parameters. Figure 11 shows an early sample whose edges and corners were degraded from handling due to the weak sintering.

Due to the poor results of the experiments at 1100°C, a third furnace was sought capable of higher temperatures. A small box furnace (manufacturer unknown) with a maximum temperature of 1200°C was used. An initial test experiment at 1200°C held for 1 hour yielded a sample with a significantly increased degree of sintering (see Figure 4). The final parameters selected for further trials included a maximum temperature of 1200°C, a hold duration of 2

hours, and ramp up/down rates of 10°C/min. Five bricks were produced, before moving to a fourth and final furnace due to availability conflicts. The remaining seven bricks were sintered using an MHI M-Series box furnace with the same parameters.

4.4. Solar AM: Solar Simulator Setup

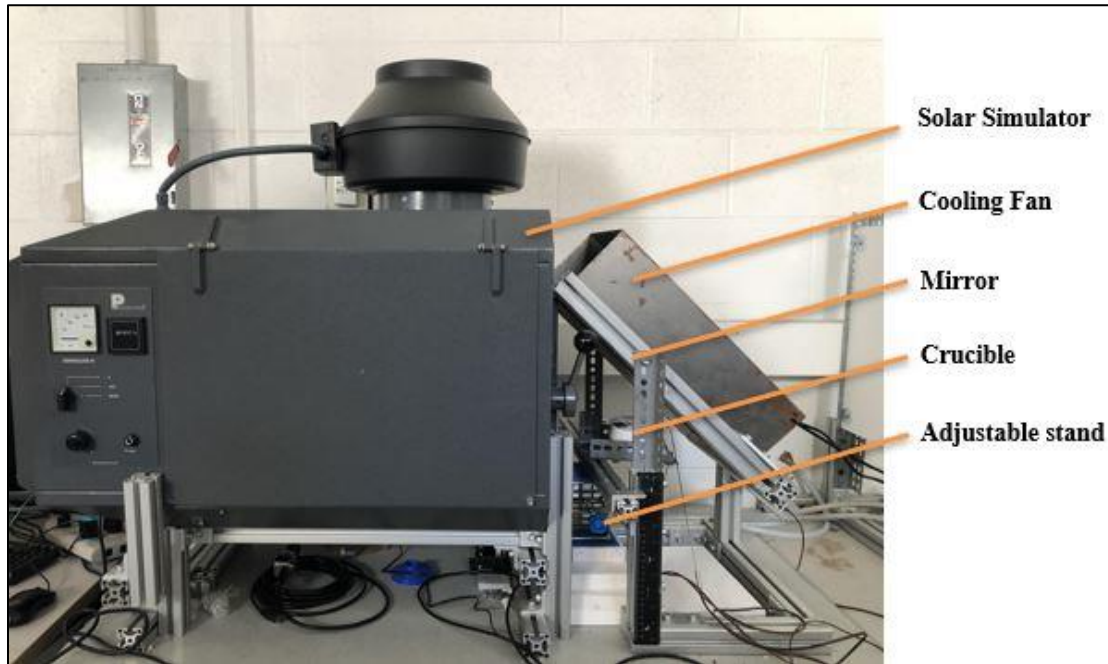


Figure 12. Solar simulator experimental setup

A high-flux solar simulator (Proyecson Xenoluxe Lamphouse 4.000/7000 W) (shown in Figure 12) was used to provide concentrated light radiation for these sintering experiments. An elliptical reflector inside the simulator, which surrounds a 7-kilowatt xenon-arc bulb, concentrates emitted light to a focal point horizontally through an aperture on the simulator. Once powered on, a lever is used to open and close the aperture. A possible current range of 60A to 200A is available for selection via a dial on the side of the simulator.

4.4.1. Solar AM: Test Stand Design

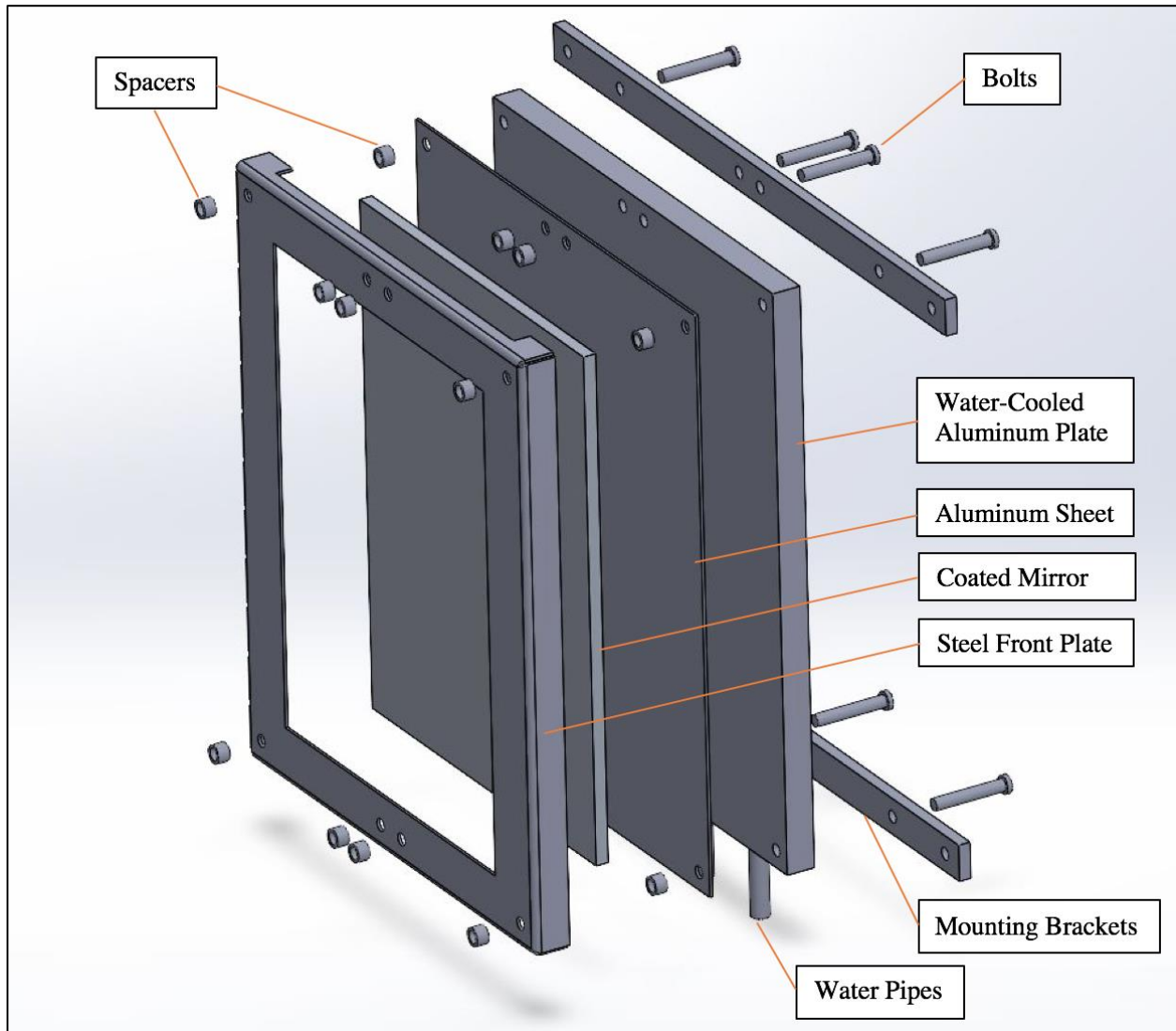


Figure 13. Exploded view of the mirror housing and water-cooling system

To sinter brick samples in consecutive layers, it was necessary to irradiate the top surface of the regolith. A test stand was designed which incorporates a water-cooled mirror to redirect the radiation beam vertically and an adjustable arm to position a crucible at the appropriate height. A full-spectrum aluminum-coated mirror (used in some commercial solar simulators) was chosen, and a pair of appropriately sized water-cooled aluminum plates were sourced.

SOLIDWORKS was used to design the steel housing and mounting system shown in Figure 13. A length of thin, high-temperature rope was fitted between the mirror and steel front plate. A thin, polished sheet of aluminum, coated on both sides with thermal paste, was placed between the mirror and the cooling plate to improve heat dissipation.

A crucible was designed to hold a cylindrical bed of regolith simulant under the beam emitted from the solar simulator. A CNC machine was used to cut a 9 cm diameter disk with a 3 cm diameter hole through its center from a 1 in thick board of alumina insulation. A second 9 cm diameter disk was cut upon which the first disk would be placed thereby creating a cavity that would hold particles. For easy height adjustment of the crucible within the beam of radiation, an adjustable stand with a rotary knob was selected.

4.4.2. Solar AM: Initial Trials

A number of test trials were conducted to determine an effective procedure and parameters for sintering bricks in consecutive layers. First, the crucible's vertical position was adjusted within the conical beam to a height where the incident light spot diameter was large enough to cover most of the simulant surface but still concentrated enough to adequately heat it to sintering temperature. Next, several different solar simulator current levels were tested across different durations of radiation exposure to determine at what point the regolith began sintering and eventually melting. Ultimately, the lowest level of available current of 60A was selected. Higher currents heated the simulant to its melting temperature too rapidly to control.

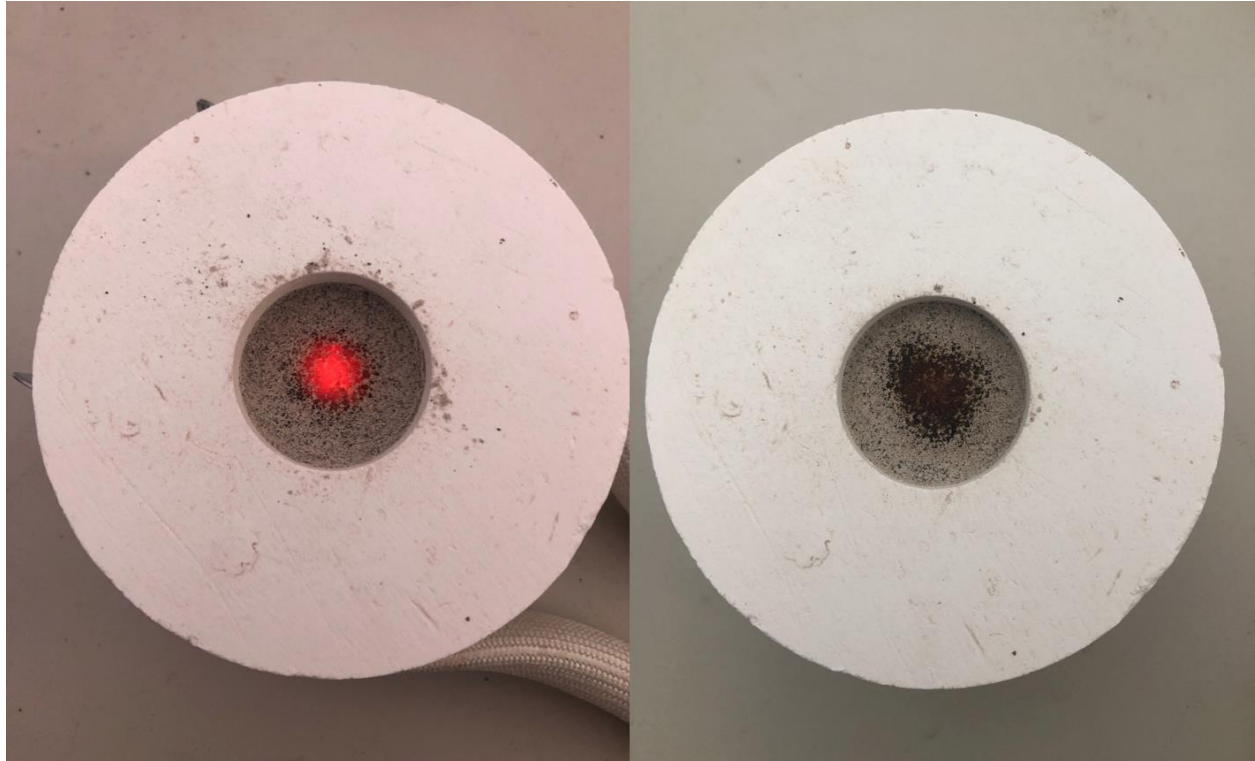


Figure 14. Crucible containing irradiated regolith simulant (left) and cooled, sintered regolith simulant (right)

Once these basic parameters were identified, the procedure for multi-layer deposition was developed. The crucible was half-filled with soil and exposed to the light beam. After approximately 90 seconds, once particles were fully sintered, the solar simulator aperture was shut. An image of the crucible immediately after removal and after the final layer had cooled is shown in Figure 14. A second layer of approximately 1 mm was deposited and tamped down using the cylindrical piece of insulation that was cut to form the crucible chamber. Tamping each new layer evenly distributes the simulant across the previous layer, improves inter-layer contact, and smooths the surfaces for improved overall brick shape. The period of layer deposition between



Figure 15. Test sample composed of 8 regolith simulant layers

sintering events was refined and reduced to approximately 15 seconds each. This was aided by calculating the exact mass of simulant corresponding to a 1 mm layer in the cylindrical crucible chamber. The second layer took approximately 1 minute and 10 seconds due to the additional heating from the layer below it. This first sample was composed of four layers. The next sample was composed of 8 layers, which is shown in Figure 15. It was obvious due to damages sustained from handling these samples that inter-layer bonding was poor. The following experiments were conducted with simulant sieved to less than 500 microns, considering that some particles were larger than the thickness of the layers themselves. Twelve samples were then produced, each with 10 1 mm layers for a final brick height of approximately 1 cm.

4.5. Brick Sample Processing



Figure 16. Furnace-sintered brick samples

Brick samples produced in the furnace required minimal processing. The samples were generally easy to remove from the silicon carbide mold but were occasionally bonded to the baseplate, requiring a firm impact to separate them. The dimensions and masses of each sample were measured and recorded. The surfaces of the samples were lightly sanded using 220 grit sandpaper to remove any minor irregularities due to packing the simulant into the mold. Furnace samples prior to any processing are shown in Figure 16.



Figure 17. Solar-AM-sintered brick samples

Once the final layer was sintered for each solar-AM brick, the crucible was left for several hours to cool. The complete sintered sample could then be removed from the surrounding un-sintered simulant. Loosely attached simulant around the perimeter of each layer was removed by hand to reveal the solid cylindrical brick. Samples at this phase are shown in Figure 17.

Attempts were made to machine the samples to more uniform dimensions first using a ceramic saw and then by hand with sandpaper. In each case, rough handling of the samples resulted in layer separation and disintegration. To prepare for strength testing, the top and bottom surfaces of each sample were lightly sanded by hand which the samples were capable of surviving.

4.6. Strength Testing Procedure

Once the samples were processed by hand, the compressive strength was measured using an MTS test system. Samples were compressed under a 50 kN load cell with an articulated head to account for slight irregularities in sample surface flatness. The load cell was driven at 1 mm/min until fracture. Load (N) versus deflection (mm) data was gathered and analyzed to determine the maximum force endured at ultimate failure. Maximum compressive strength was calculated from this maximum force and the samples' cross-sectional area. Digital calipers were used to measure the rectangular samples' width and depth and the cylindrical samples' diameters for this calculation.

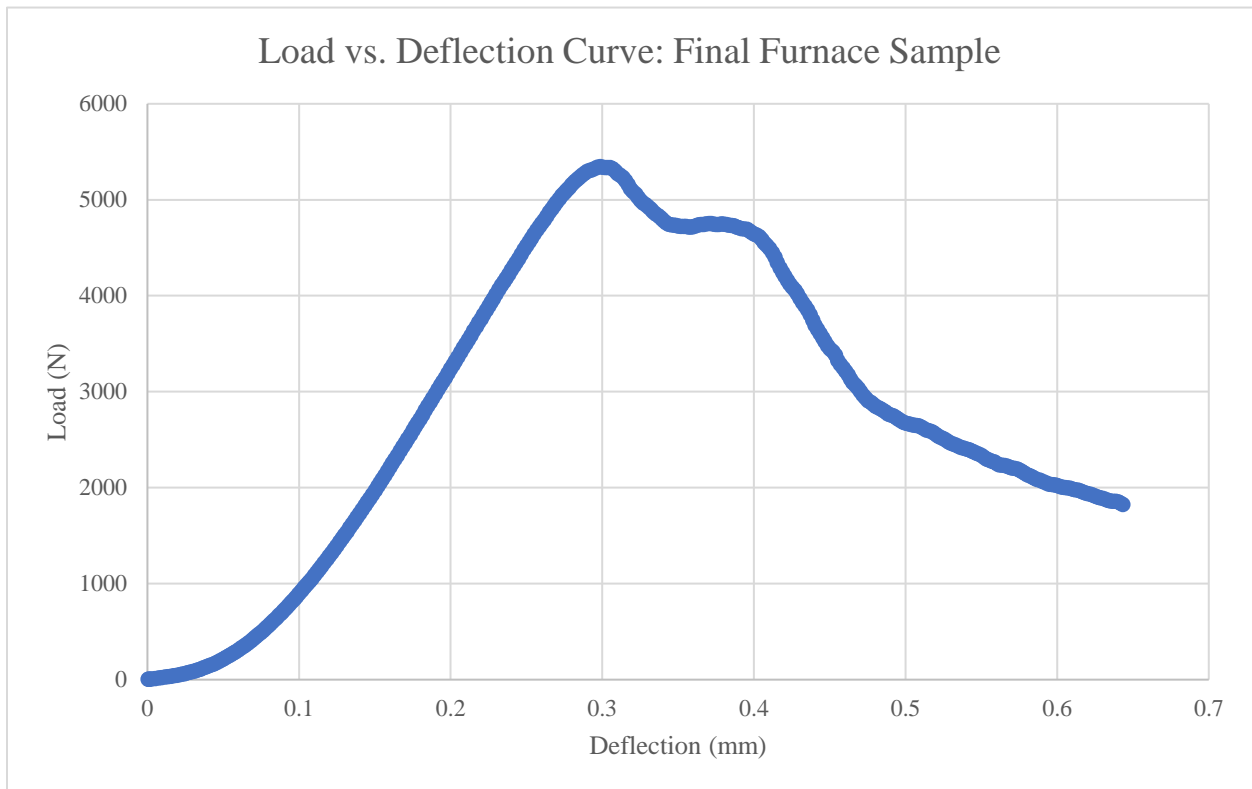


Figure 18. Representative final furnace sample load vs. deflection curve

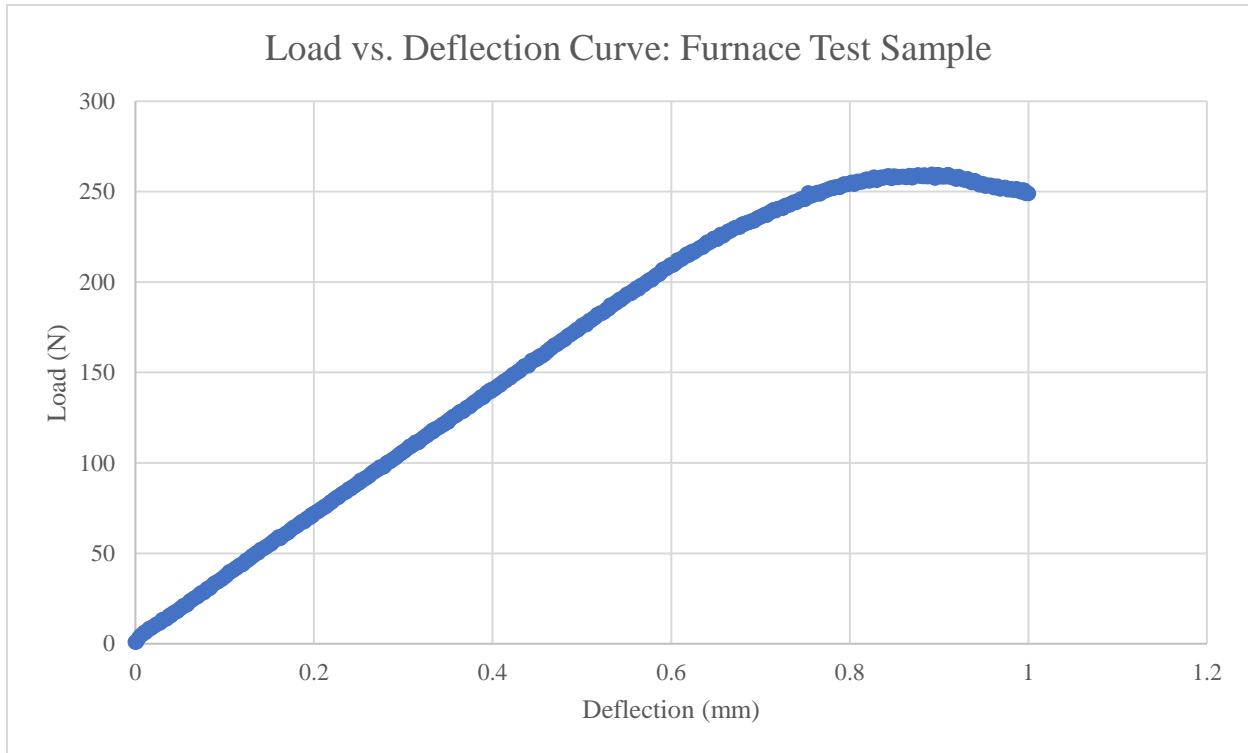


Figure 19. Representative test furnace sample load vs. deflection curve

Figure 18 shows an example of the plotted load vs. deflection data for a furnace-sintered final sample. Secondary fractures were common due to settling of large fragments following ultimate failure which were still capable of supporting a significant load. A notable feature of these data were the initial nonlinear sections prior to the linear-elastic regime below about 0.1 mm. This is most likely due to settling of the articulated load cell head which would have compressed slightly before the sample was fully engaged. Figure 19 shows a load-deflection curve of one of the test samples from early sintering trials. Apart from the significantly lower loads, a notable difference seen in these curves is the smooth, simple profile compared to the curve in Figure 18. The lower temperatures of these initial trials produced a softer sintered material which compressed like compacted sand in that its failure was gradual but complete. No smaller fragments could support secondary loads.

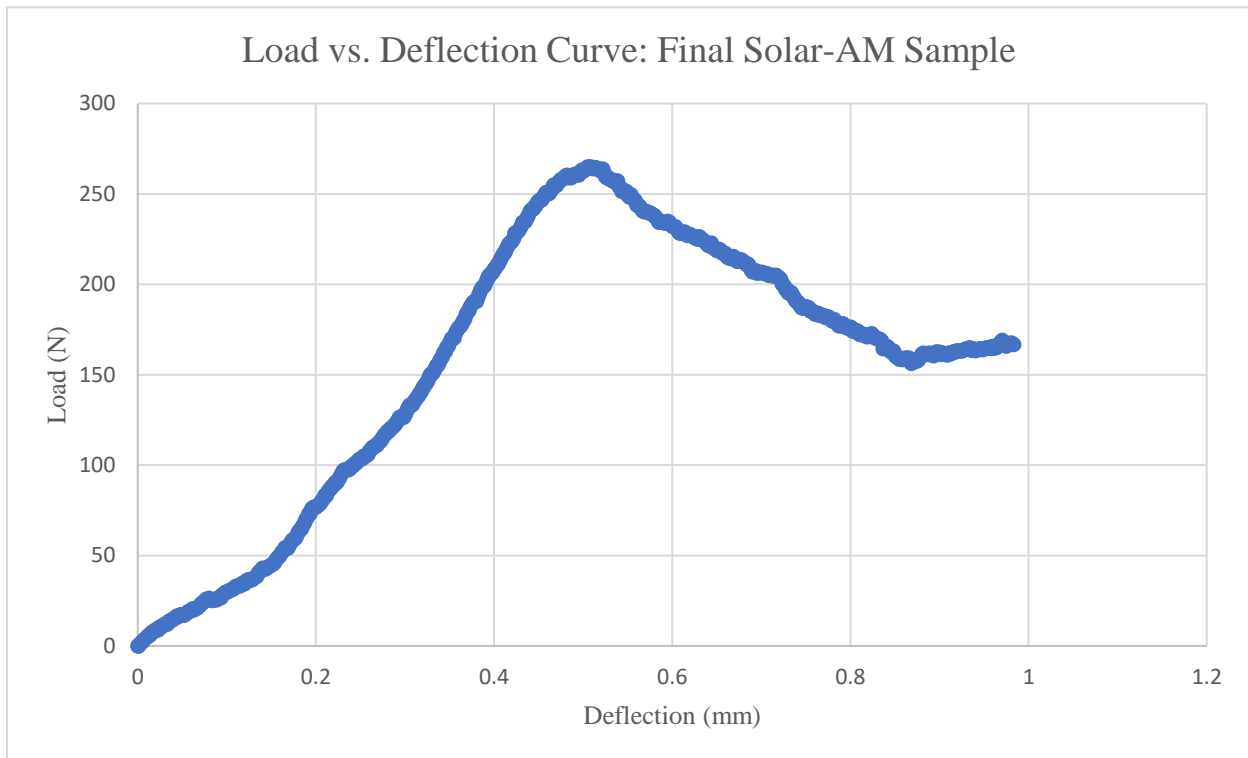


Figure 20. Representative final solar-AM sample load vs. deflection curve

As seen in Figure 20, the data from the solar-AM samples produced irregular curves. The failure point is still easily determined, but the pre-failure regime is far less linear than any of the furnace samples. There are two main reasons that may have caused this unevenness. First, despite efforts to post-process the samples by hand, it is unlikely that the top and bottom faces of the samples were entirely parallel. The furnace samples were also lightly post-processed, but the surfaces were far more even due to being contained in a rigid mold. Second, sintering with direct solar energy caused significant thermal gradients both radially (between the center of the beam which has the highest light concentration and the edge of the light spot which is much dimmer) and vertically through the layers. Both circumstances allow for a high possibility of internal stress formation and thermal cracking. These mechanisms may account for both the low

compressive strength of the samples and the irregular load-displacement curves as seen in Figure 20.

Another potential influence for the high level of noise in the solar-AM curves may be the nonlinear behavior of the settling compressive test rig discussed previously. This nonlinear section occurs below about 800 N, and is pronounced in Figure 18 because the curve extends to over 5000 N. However, the entire curve in Figure 20 does not exceed 300 N. The test system settling may cause noise in all curves below 800 N loads.

4.7. Compressive Strength Results

Table 7 shows data corresponding to the initial test trials of the furnace sintering experiments discussed in section 4.3.1. Each of these samples were sintered at a maximum hold temperature of 1100°C.

Table 7. Furnace sintering test experiment data

Test Sample #	Furnace Number	Hold Duration	Sample Characteristics	Max Compressive Strength (MPa)
1	1	10 Mins	Large temp variation due to poor controller. Sample bottoms rough and barely sintered.	1.94
2	1	10 Mins		1.54
3	2	20 Mins	Increased sintering. Some simulant sticking to SiC walls. Weak edges.	1.86
4	2	30 Mins	Roughly the same. Bottom face has improved sintering.	1.79
5	2	60 Mins	No noticeable difference.	0.51
6	2	10 Hrs	No significant difference. Bottom SiC plate fused to sintered material.	0.93
7	2	60 Mins	¼ thickness sample to test sintering depth. No noticeable difference.	Inconclusive

Table 8 and Table 9 show the complete measured data of the bricks from the furnace experiments and solar-AM experiments, respectively. The solar-AM samples were smaller and less regular, but the biggest difference was in compressive strength which was found to be significantly lower. There are some noticeable irregularities in the furnace-sintered bricks. Samples A4-A8 were sintered in the third high-temperature furnace, and sample F1-F7 in the fourth and final furnace as discussed in section 4.2.1. Despite the parameters of the two furnaces being nearly identical (maximum temperature, heating profile, etc.), the compressive strengths of samples sintered in the final furnace are notably higher. This is likely due to the more stable heating profile of the MHI box furnace. Furthermore, “A” samples used approximately 6 grams of simulant whereas “F” samples used precisely 6 grams of simulant prior to sintering. The strength testing procedure was identical for all samples.

Table 8. Final furnace-sintered brick measurements

Furnace Sintering								
Sample	Width (mm)	Length (mm)	Height (mm)	Volume (mm³)	Mass (g)	Area (mm²)	Max Force (N)	Max Strength (MPa)
A4	15.46	16.85	14.21	3701.7	6.7	260.5	2946	11.31
A5	15.22	16.89	14.5	3727.5	6.6	257.1	3226.8	12.55
A6	15.37	16.7	14.55	3734.7	6.9	256.7	3582.6	13.96
A7	15.42	16.71	12.82	3303.3	5.8	257.7	2125.7	8.25
A8	15.13	16.64	14.7	3700.9	6.5	251.8	2345.2	9.32
F1	15.25	17.38	12.17	3225.6	5.8	265.0	4253.7	16.05
F2	14.93	16.47	12.87	3164.7	5.9	245.9	4872.7	19.82
F3	15.22	17.42	12.26	3250.5	5.8	265.1	3998.3	15.08
F4	14.75	16.45	12.86	3120.3	5.9	242.6	5343.8	22.02
F5	15.01	16.42	12.51	3083.3	5.8	246.5	3998.2	16.22
F6	15.33	16.77	11.98	3079.9	5.8	257.1	5284.9	20.56
F7	15.52	17	12.09	3189.8	5.9	263.8	4042.1	15.32

Table 9. Final solar-AM-sintered brick measurements

Solar AM Sintering							
Sample	Diameter (mm)	Height (mm)	Volume (mm ³)	Mass (g)	Face Area (mm ²)	Max Force (N)	Max Strength (MPa)
S1	13.46	9.59	1364.6	1.9	142.3	265	1.862
S2	14.45	7.94	1302.1	1.8	164.0	447.7	2.730
S3	15.11	10.2	1829.0	2.2	179.3	208.7	1.164
S4	14.2	10.07	1594.8	2.2	158.4	172.3	1.088
S5	14.12	9.18	1437.5	1.9	156.6	268	1.711
S6	15.32	8.65	1594.5	1.8	184.3	295.3	1.602
S7	14.97	10.2	1795.3	2.1	176.0	214.4	1.218
S8	14.29	8.59	1377.7	1.8	160.4	221.9	1.384
S9	14.35	7.06	1141.8	1.6	161.7	466.8	2.886
S10	16.54	6.54	1405.2	1.6	214.9	408.4	1.901
S11	13.54	6.99	1006.5	1.3	144.0	285	1.979

4.8. Elasticity Calculation

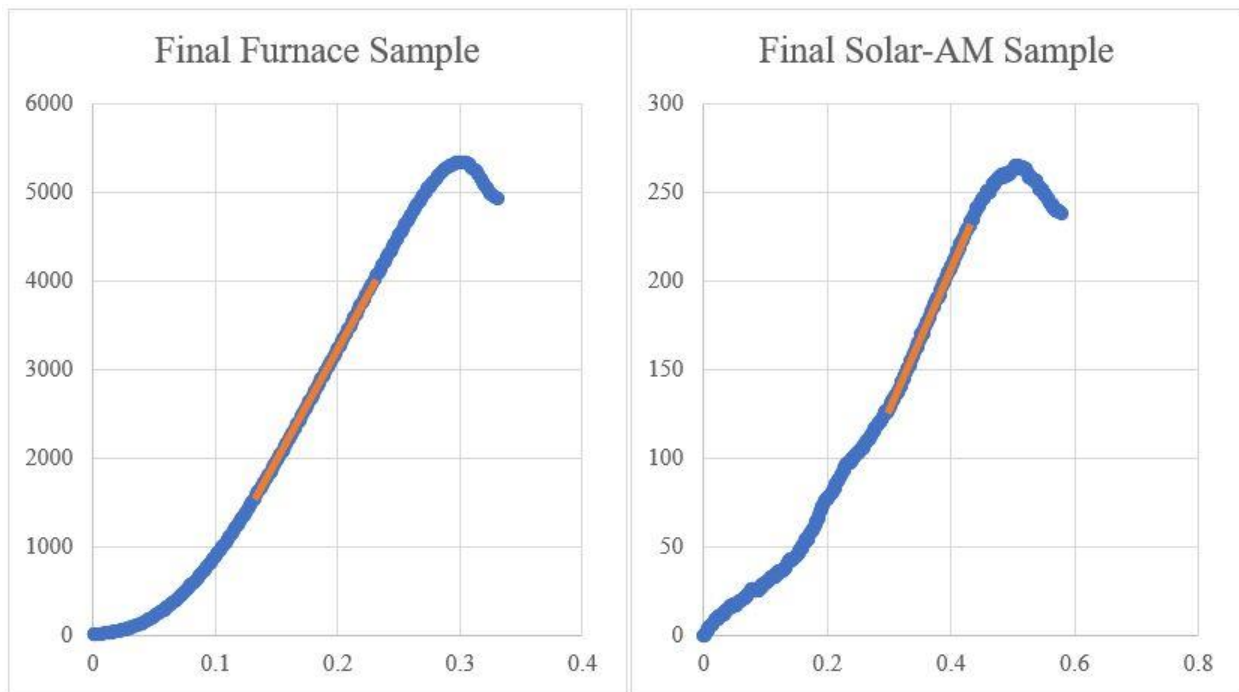


Figure 21. Truncated load-deflection curves with linear-elastic slope approximations

The Young's modulus of each sample was calculated by approximating the slope of the linear-elastic portions of the respective load-deflection curves. Individual data points were selected from both ends of the most linear section and the slope was calculated using the point-slope formula. Representations of the slope determinations are shown in Figure 21 on truncated versions of the representative curves from Figure 18 and Figure 20. The values obtained are shown in Table 10 and are consistent with the findings in other studies.

4.9. Compressive Strength Consistency in Prior Research

Table 10. Average compressive strengths, strength standard deviations, and average Young's Moduli per method

Method	Average Compressive Strength (MPa)	Standard Deviation (MPa)	Average Young's Modulus (GPa)
Furnace	15.0	± 4.3	18.6
Solar-AM	1.78	± 0.6	0.89

As discussed in section 2.3.1, radiant furnace experiments have yielded samples with very high compressive strengths, some over 200 MPa. It is important to consider the variables that may be at work in producing such high strengths, such as particle size, cold-pressing pressure, and simulant type. To recap, the radiant furnace experiments in this research sintered as-is LHS-1 simulant in air, with no cold or hot pressing. The maximum hold temperature was 1200°C for 2 hours. There are several studies whose experimental parameters align closely to these. Allen et al. used a slightly lower maximum temperature with a range of hold durations from 0.17-72 hours. The resulting samples compressive strengths were between 2.8 and 26 MPa [109]. Another study by Allen, with very similar experiment parameters to this research except a lower maximum temperature reported a maximum compressive strength of 7.6 MPa [110]. Hoshino et al., despite sintering in a vacuum, had comparable maximum temperatures and hold

durations from 0.17-1 hour. These samples had compressive strengths between 33 and 38 MPa [72]. Fateri et al. sintered samples at 1120°C for 3 hours producing a maximum compressive strength of 13 MPa [111]. The studies with the closest experimental parameters to those in this research all report comparable maximum compressive strengths.

Section 2.3.4 discusses several additive manufacturing studies. Very few studies have combined AM technology with concentrated solar energy. Previously mentioned was the study by Meurisse et al. whose solar-3D printed sample yielded a compressive strength of 2.3 MPa [85]. The only other compressive strength data from a solar-AM study is provided by Fateri who reported a strength of 2.5 MPa [112]. Despite the limited reference data, these two studies report very similar maximum compressive strength results for solar-AM experiments.

CHAPTER 5

APPLIED USABILITY CRITERIA

5.1. Method Usability Evaluation

The intent of the following evaluation is to demonstrate the application of the Usability Criteria as an evaluation tool and to highlight some fundamental differences between two of the most prominent sintering methods. As evident in the sections presenting the Usability Criteria, many of the assessment characteristics are intended for full-scale systems as opposed to laboratory setups. Some assumptions and modifications will be made to account for this. Therefore, final grades given to these methods themselves will not carry a significant value apart from differentiating between the two methods. In the future, the Usability Criteria can be adjusted, new parameters may be added, and the significance of the final grades will be improved thereby aiding in the method testing and selection process for full-scale systems.

5.2. Sample Grading and Discussion

The most obvious difference between the furnace-sintered and solar-AM-sintered samples is the resulting brick shape. These shapes were selected to minimize complexity. Bricks tend to generally have rectangular geometry, and for furnace sintering, the difficulty of machining silicon carbide made other mold geometries impractical. For solar-AM sintering, rectangular crucible geometries were considered but both the difficulty of machining sharp corners with a CNC milling machine and the circular coverage of the incident radiation led to the chosen cylindrical crucible. Had it been possible to produce samples of significantly larger diameter and higher strength, post-processing of the slightly irregular cylinders into cleaner rectangular bricks would have been pursued. With regards to brick size, the mold used in the

furnace could likely be made larger to an extent, until the heat no longer penetrates deep enough to sinter the entire thickness of the brick. This is when supplemental hybrid microwave sintering can be used, as discussed in section 2.4.3, by heating the brick internally. A furnace-sintered brick was bisected to determine the sintering depth and it was concluded that at this size the brick sintered fully throughout. The primary size limitation for the Solar AM bricks is the diameter of the incident radiation. More layers can easily be applied to build a taller brick, but without multiple beams or the ability to move the beam across the simulant surface, the brick diameter (or width) is constrained.

While the samples are similar in terms of volume and maximum dimensions, the biggest difference evident in the data is the compressive strengths. As discussed in Chapter 2, furnace sintering consistently outperforms additive manufacturing and direct solar sintering in terms of compressive strength. The primary reason for this difference is the consistent and controlled heating profile provided by electric furnaces which eliminates thermal cracking often experienced by samples produced with a direct radiation beam. The solar AM samples in this study underwent repeated heating and cooling across consecutive layers. Furthermore, despite efforts to improve inter-layer bonding as discussed in section 4.4.2, there was still poor adhesion between the solar AM sample layers. Previous studies have used layers of approximately 1 mm with some success, but others suggest maximum layer thicknesses less than 0.1 mm for complete inter-layer sintering [58] [75]. To achieve the same brick size at this layer thickness would require 100 layers and considerably more manual labor. It has been shown that sieving regolith, which results in a lower porosity, can achieve higher sintered compressive strength when other variables are accounted for [69]. However, any potential strength improvement by sieving the

simulant for the solar AM trials was negligible against the losses due to thermal cracking and poor layer bonding.

5.2.1. Compressive Strength

Furnace Sintering

Grade: 3

The average compressive strengths of the bricks were found to be 11.08 (± 2.3) MPa for “A” samples and 17.87 (± 2.8) MPa for “F” samples: a difference discussed previously that may be due to controller quality between furnaces. Across all twelve furnace samples the average strength is 15.04 (± 4.3) MPa. Each of these averages represents a grade of 3 in the strength category, suggesting that this sintering method would produce material “sufficient for most Lunar applications”.

Solar-AM Sintering

Grade: 1

Across the eleven solar-AM samples the average compressive strength was found to be 1.78 (± 0.6) MPa. Strength improvements can be made (decreasing grain size, reducing thermal gradients, etc.) to this method and will be a critical element for full-scale system development, but it is unlikely to outperform the stable sintering process of the furnace. At this strength, the material can be crushed or pulverized by hand making it a “poor structural material”.

5.2.2. System Versatility

Furnace Sintering

Grade: 2

The first parameter relating to versatile outputs regarding furnace sintering is the size of the heating chamber. Each furnace used in this research from test trials through final sample production had a different chamber size, but ultimately, the size and shape of each sample is limited by this dimension. The second limitation is the geometry of the high-temperature mold. In this research, the difficulty of machining silicon carbide led to the simple cubic geometry. Even with advanced machining techniques and materials, a separate mold is required for each desired shape.

It is difficult to predict the versatility of a full-scale furnace system, but the same general constraints will likely remain including chamber size and mold shape. A Lunar furnace would likely be large and complex for protection against the harsh environment and considering the necessity for large-scale samples. Furthermore, it would need to remain near electrical sources (or require heavy solar-compatibility equipment) and would therefore be immobile. A reasonable conclusion would be that at best, a full-scale system would have “low versatility”.

Solar-AM Sintering

Grade: 4

Laboratory versions of solar additive manufacturing have a variety of serious drawbacks and limitations. The main constraints in this research were the crucible geometry and incident

radiation area discussed in section 4.4.2. To sinter larger-area layers, both the crucible size and the surface radiation exposure would need to be adjusted. An entirely new system would need to be designed such as a translating crucible bed or movable radiation beam. The vertical dimension, however, is easily adjustable. A custom crucible may be needed to account for samples with significantly increased height, but the same sintering procedure would be used.

Full scale Lunar 3D printing architecture is still in its infancy, but basic designs are offered in renditions like the example in Figure 9. The central goal of additive manufacturing is rapid, versatile production. At all levels, additive manufacturing will outperform furnace sintering in terms of versatility. These qualities will be maintained in full scale Lunar systems and will therefore be considered for this evaluation as having “high versatility”.

5.2.3. Energy Cost per Unit Volume

Furnace Sintering

Grade: 4

Full-scale furnace designs for Lunar implementation have not yet been proposed, but it is certain that the laboratory furnaces used in this research are far from optimized for this application. The MHI box furnace is capable of reaching 1400°C with a chamber size of 12 in. x 12 in. x 16 in.: far larger than the brick samples. A simple heat loss analysis was conducted to estimate the energy used by the furnace during the four-hour trials. The six-gram samples of simulant required approximately 5,664 J of energy to reach the 1200-degree maximum temperature. Considering the 55 kJ of energy required to heat the air in the chamber, the approximate 632 W lost through the furnace walls at peak temperature, and the average sample

volume of 3.36 cm^3 , the energy usage was found to be approximately 1.35 MJ/cm^3 . If three samples are sintered simultaneously, which the chamber size can permit, this usage drops to 451 kJ/cm^3 .

For a more useful comparison, the energy efficiency of a full-scale version of the laboratory setup is estimated. The largest box furnace from the same manufacturer provides a chamber size much closer to the scale needed for habitation-grade structural brick sizes (16 in. x 24 in. x 24 in.). A brick size of 12 in. x 20 in. x 20 in. and a sintering period of 10 hours to account for the significantly increased brick thickness are assumed. Approximately 96.5 MJ are required to heat this volume of simulant and over 104.6 kJ to heat the air in the chamber (the assumed medium for heat transfer). Over ten hours, approximately 55 MJ of heat may be lost through the insulation with the same characteristics as the laboratory system. The energy efficiency of this full-scale system approaches the theoretical maximum at just 1.93 kJ/cm^3 . This hypothetical system would achieve a grade of 4.

Solar-AM Sintering

Grade: 3

Full-scale additive manufacturing systems for Lunar implementation have only been digitally rendered, but again the laboratory setup here ignores energy efficiency. At the desired 60 A current setting the solar simulator was using approximately 7.2 kW during these experiments. The average experiment duration to sinter a 10-layer sample was 24.7 minutes. While the simulator aperture was closed for approximately 15 seconds between each layer, it

remained on. Considering an average sample volume of 1.44 cm^3 , the energy usage was found to be approximately 7.41 MJ/cm^3 .

The paper by Physical Science Inc. discussed in section 2.3.4 used a solar concentrator and fiber optic rod to sinter volcanic soil [83]. Approximately 540W of solar was the estimated power used for sintering, which will be the assumed substitute for electricity in this solar-AM system. In this research, 10 layers were sintered per sample with an average layer area of 167.4 mm^2 for a total sintered area of $1,674 \text{ mm}^2$. The aforementioned concentrated solar power was capable of sintering approximately $0.6 \text{ cm}^2/\text{s}$, giving a sintering time of just 28 seconds per 10-layer sample. An average period of 15 seconds was necessary for each layer deposition in this research. Assuming an improved system has automated this procedure to just 3 seconds between layers, a reasonable estimate for total sintering time is approximately 55 seconds. Considering the average sample volume of 1.44 cm^3 , this improved system may achieve an energy efficiency of approximately 20.5 kJ/cm^3 , or a grade of 3.

5.2.4. Labor Requirement

Furnace Sintering

Grade: 2

While furnace sintering takes significantly longer to produce samples than solar-AM due to the constrained heating and cooling rates, the entire heating profile is accomplished without operator interference. While this may be considered autonomous, at least for the sintering duration, the pre- and post-sintering intervention is not simple. As discussed in section 4.2, new mold-securing clips had to be fabricated for each experiment and the mold needed to be filled

and packed carefully to ensure uniformity. After sintering, the samples were removed, and the silicon carbide plates were sanded by hand to remove any bonded simulant. Under the Usability criterion, two qualities are met under grade 2 (b and c): more than any other. While there is no monitoring required during sintering (2-a), the system is far from autonomous for construction applications.

Solar-AM Sintering

Grade: 3

The solar-AM method applies well to the description: “manually operated”. An operator is required for initialization (massing, crucible-filling, tamping, height adjustment), solar simulator aperture operation, layer deposition, visual sintering inspection and timing, and sample removal and processing. At laboratory scale, each quality of grade 1 is met.

It is reasonable to assume that full-scale Lunar additive manufacturing systems will aim for full automation during sintering and construction. Without a clear understanding of the specific qualities a full-scale system would meet, it can at least be assumed that a solar-AM system would require less labor than a furnace system. For this evaluation, the solar-AM method will be considered “low labor”.

5.2.5. Production Rate and Mass Efficiency

Production rate and mass efficiency focuses primarily on equipment rather than the sintered product. Considering the small scale of the laboratory equipment used in this research, its analysis will not yield useful results for an initial stage Lunar development application. The

point of this evaluation is to compare the two methods, and a discussion is provided differentiating the two methods including estimated scores. It will be assumed that energy collection methods are the same and are omitted from analysis.

Furnace Sintering

Grade: 2

The furnace experiments, with the ability to sinter multiple samples simultaneously, had a production rate of approximately 1.53-4.58 g/hr. Although a full-scale system would have a much higher sintering rate, the rate of this method will be considered “gradual”. While an exact mass is difficult to estimate, it is reasonable to assume that a furnace capable of sintering full-scale Lunar bricks – including a large, likely air-filled chamber, and either a resistance heating element or fluid heat exchanger (in the case of using solar-heated fluid) – would be of considerable mass. For this evaluation, a hypothetical furnace system will be considered in the “standard” mass category.

Solar-AM Sintering

Grade: 4

The solar-AM method produced sintered material at a rate of approximately 4.47 g/hr. Like the furnace analysis, a full-scale advanced manufacturing system would have a much higher sintering rate. Considering that AM technology is among the fastest in terms of production (fabrication of structures/structural material), in this analysis it will be categorized as

“moderate”. Lunar regolith does not require containment for sintering using AM. In the designs discussed previously, theoretical systems rely on robotics to sinter larger samples. For this analysis, a hypothetical solar-AM system will be considered “lightweight” equipment.

5.3. Matrix Evaluation

Throughout this evaluation, a series of reasonable estimates and assumptions were made depending on availability of data and information. No data was collected nor were estimates yet made for the hardness or uniformity categories, but their importance factors (1 and 2, respectively) reflect that they may not ultimately be important criteria. The assessments with the highest level of confidence are strength and labor requirement, considering that this data was easily accessible. There is moderate confidence in the versatility assessment despite the lack of full-scale system knowledge. Due to the high level of estimation involved in the energy requirement and production rate and mass efficiency categories there is not a high level of confidence in their grades. However, the evaluation was shown to be useful in distinguishing performance between the two methods and their sintered products, and the solar-AM sintering method ultimately scored higher in overall usability. Final scores are tabulated in Table 11.

Table 11. Usability Criteria score matrix

Usability Criteria	Weight	Furnace Method	Solar-AM Method
Strength	4 (.8)	3	1
Hardness	1 (.2)	-	-
Versatility	4 (.8)	2	4
Energy Cost per Unit Volume	5 (1)	4	3
Labor Requirement	3 (.6)	2	3
Uniformity	2 (.4)	-	-
Production Rate & Mass Efficiency	4 (.8)	2	4
Total		10.8	12

CHAPTER 6

CONCLUSION AND FUTURE WORK

6.1. Conclusion

Not only is there a significant attraction to and motivation for returning to the Moon, but the public and private sectors are well underway in establishing Lunar infrastructure and the first steps into a space industry. ISRU, primarily the utilization of Lunar regolith, will be a critical component of successful settlement of the Moon. Regolith sintering will likely be employed as a construction method for much of the necessary Lunar infrastructures such as habitats, roads, landing pads, and bridges.

To help close the gap between laboratory scale research and usable, implementable systems for Lunar construction, a set of seven criteria were proposed constituting the most important considerations for sintering systems and properties of sintered material. Among the most important categories identified were energy efficiency (system), strength (material), and a combination of production rate and mass efficiency (system). Two categories, hardness and uniformity (material), were included as potentially important criteria, but due to limited attention in the relevant literature no grading scheme is yet proposed. It may be found that the hardness of sintered regolith is of little concern for construction on the Moon, but more research is encouraged. However, standards for acceptable uniformity of sintered regolith will surely be required in the future in some form. This research also replicated two promising sintering methods at laboratory scale: furnace sintering and solar additive-manufacturing. The two methods represent various strengths and weaknesses of the current state of regolith sintering technology, and the samples produced are consistent with existing research. The usability criteria were used to evaluate the methods to highlight these differences. The key areas where the

methods deviated were compressive strength, versatility, and production rate and mass efficiency. Additive manufacturing technology is defined by its rapid build rate and versatile construction, but this evaluation helped emphasize that for sintered regolith, the cost of production rate is strength with just 11.8% the average compressive strength of the furnace-sintered bricks. The deviation in the remaining scores was less significant but the solar-AM method consistently outperformed the furnace method in the system efficiency categories. Still, it should be noted that laboratory-scale experiments are not the intended application for this evaluation. The usability criteria are a novel assessment for Lunar sintering systems and, with refinement, may be beneficial for guiding both future research and the selection process for full-scale sintering systems.

6.2. Future Work

The two sintering methods replicated in this study provided unique challenges and lessons for future research. For furnace sintering, there was difficulty producing a fully-sintered sample at first, and it should be noted that in general a high-quality controller is important for ensuring precise heating and cooling regimes, and that for LHS-1 simulant, complete sintering occurs at 1200°C. Furthermore, while silicon carbide has excellent thermal properties, it was found to consistently bond to particles of LHS-1 during sintering making it difficult to remove samples from the mold. Bonding increased after each consecutive experiment, requiring new molds to be fabricated after approximately 8 uses. Graphite may be a suitable substitute mold material. For the solar-AM experiments, perhaps the greatest weak point was strength which is likely due to the poor inter-layer bonding. In the future, thinner layers with adjusted (sieved) particle sizes should be tested to determine if strength can be increased. Experiments in this study were limited by the size and shape of the crucible and the shape of the concentrated-light

beam. Furthermore, efforts should be made to reduce the thermal gradients induced by the concentrated light beam and the layer deposition periods. Future research should test different beam configurations, diameters, and intensities to optimize sintering.

In general, the Usability Criteria will require refining and will benefit from developments in sintering technology, progression in Lunar base architecture and planning, rocket technology, and other adjacent fields. It is possible that new criteria may be introduced, and current criteria removed as scientists gain a better understanding of sintered regolith construction requirements.

Compressive strength is one of the better understood properties of sintered regolith, but it is still likely that a more appropriate grading scheme can be developed in the future. The proposed scale ranges from less than 2 MPa up to 300 MPa. It may be the case that there aren't any structural applications of sintered regolith below 25 MPa and that other system limitations make it impractical to produce sintered regolith above 200 MPa (e.g. energy efficiency). In this case, these new boundaries for the grading scheme, as well as more appropriate intermediate strength ranges, can be established.

Hardness is in general an important material property, but far more research is needed as it pertains to sintered regolith to understand its role in structural applications. It will be beneficial to know what sintering parameters affect hardness (if any), and what other applications might become available with a known hardness profile. Materials with high hardness tend to be highly brittle, so a better understanding of sintered regolith hardness may be crucial for risk mitigation when designing Lunar structures. Alternatively, if a consensus is reached on sintered regolith hardness which can't easily be altered, there may be no need for a Usability category or grading scheme for hardness.

As sintering and construction technology improve, the definitions of Versatility, Labor Requirement, and Uniformity will likely evolve. For instance, if all sintering systems contending for Lunar construction are fully autonomous, the Labor Requirement criterion will be reduced to just the “Fully Automated” category which can then be expanded to incorporate differences between these systems. The same is true for versatility if all contending systems are based on additive manufacturing technology. As sintering systems improve, a full category for uniformity may be unnecessary, but it is likely that some measure of brick/product consistency and quality would be beneficial.

Energy efficiency is largely missing from regolith sintering studies. The first step in improving energy efficiency understanding will be the widespread reporting of data in future studies. This data should follow the same kJ/cm^3 unit standard used in this work for simpler comparison. As sintering technology progresses towards full-scale systems, it will be important to include a more comprehensive analysis of energy efficiency including energy production methods, mass of equipment, and cost of technology. As mission plans become solidified and the energy capacity of early Lunar bases becomes more well-defined, a more accurate grading scheme can be implemented for sintering systems.

Finally, only rough estimates have been produced for full-scale systems in the production rate and mass efficiency category. This criterion can be adjusted once the capabilities of full-scale systems are realized. Attempts should be made in future research to improve production rate, and it should become standard to report production rate data. For furnace sintering, larger samples should be made to determine the maximum amount of regolith that can be sintered in a given period. For solar-AM methods, refining the layering procedure with automated systems

will significantly improve production rate. Furthermore, larger rockets will relax the limitations on mass transport, widening the possibilities for full-scale systems.

BIBLIOGRAPHY

- [1] I. Crawford, "Introduction to the Special Issue on using extraterrestrial resources to facilitate space science and exploration," *Space Policy*, vol. 37, p. 51, 2016.
- [2] M. Marov and E. Slyuta, "Early steps toward the lunar base deployment: Some prospects," *Acta Astronautica*, vol. 181, pp. 28-39, 2021.
- [3] A. Meurisse, "Preface to the special issue on "Space resources"," *Planetary and Space Science*, vol. 185, no. 104894, 2020.
- [4] M. Palos, P. Serra, S. Fereres, K. Stephenson and R. Gonzalez-Cinca, "Lunar ISRU energy storage and electricity generation," *Acta Astronautica*, vol. 170, pp. 412-420, 2020.
- [5] "Every Mission to the Moon, Ever," The Planetary Society, 2023. [Online]. Available: <https://www.planetary.org/space-missions/every-moon-mission>. [Accessed 13 February 2023].
- [6] H. H. Schmitt, *Return to the Moon*, New York: Praxis Publishing Ltd, 2006.
- [7] J. Carpenter, R. Fisackerly and B. Houdou, "Establishing lunar resource viability," *Space Policy*, vol. 37, pp. 52-57, 2016.
- [8] European Space Agency, "Helium-3 mining on the lunar surface," ESA, [Online]. Available: https://www.esa.int/Enabling_Support/Preparing_for_the_Future/Space_for_Earth/Energy/Helium-3_mining_on_the_lunar_surface. [Accessed 14 March 2023].
- [9] A. Kleinschneider, "Feasibility of lunar Helium-3 mining," in *40th COSPAR Scientific Assembly*, Moscow, Russia, 2014.
- [10] E. Stoll, P. Harke, S. Linke, F. Heeg and S. May, "The regolith rocket—A hybrid rocket using lunar resources," *Acta Astronautica*, vol. 179, pp. 509-518, 2021.
- [11] N. Bennet, D. Ellender and A. Dempster, "Commercial viability of lunar In-Situ Resource Utilization (ISRU)," *Planetary and Space Sciences*, vol. 182, no. 104842, 2020.
- [12] SpaceX, spacex, 2023. [Online]. Available: <https://www.spacex.com/>. [Accessed 12 February 2023].
- [13] L. Grush, "Asteroid-Mining Startup AstroForge to Launch First Space Missions This Year," Bloomberg L.P., 24 January 2023. [Online]. Available:

- <https://www.bloomberg.com/news/articles/2023-01-24/asteroid-mining-startup-astroforge-plans-first-platinum-refining-space-missions>. [Accessed 12 February 2023].
- [14] "Lunar Resources," Lunar Resources, 2023. [Online]. Available: <https://www.lunarresources.space/#about>. [Accessed 1 December 2022].
- [15] "Lunar Outpost," Lunar Outpost Inc., 2023. [Online]. Available: <https://lunaroutpost.com/>. [Accessed 1 December 2022].
- [16] M. Lou and B. Giggs, "NASA wants to land astronauts on Mars by 2033," 3 April 2019. [Online]. Available: <https://www.cnn.com/2019/04/03/us/nasa-mars-mission-2033-scen-trnd/index.html>. [Accessed 13 February 2023].
- [17] NASA, "Gateway Domestic and International Benefits-Memo," 2 May 2018. [Online]. Available: https://www.nasa.gov/sites/default/files/atoms/files/gateway_domestic_and_international_benefits-memo.pdf. [Accessed December 2022].
- [18] G. Jordan, "Mars Ep. 4: Deep Space Transport," NASA, 27 January 2023. [Online]. Available: <https://www.nasa.gov/johnson/HWHAP/mars-ep4-deep-space-transport>. [Accessed 30 January 2023].
- [19] S. Xu, "China Plans to Build Nuclear-Powered Moon Base Within Six Years," Bloomberg L.P., 5 November 2022. [Online]. Available: <https://www.bloomberg.com/news/articles/2022-11-25/china-plans-to-build-nuclear-powered-moon-base-within-six-years#xj4y7vzkg>. [Accessed 16 February 2023].
- [20] B. Lehner, "Human Assisted Robotic Vehicle Studies - A conceptual end-to-end mission architecture," *Acta Astronautica*, vol. 140, pp. 380-387, 2017.
- [21] P. Metzger and G. Autry, "The Cost of Lunar Landing Pads with a Trade Study of Construction Methods," University of Central Florida, Orlando, 2022.
- [22] J. Rasera, J. Cilliers, J. Lamamy and K. Hadler, "The beneficiation of lunar regolith for space resource utilisation: A review," *Planetary and Space Science*, vol. 186, no. 104879, 2020.
- [23] NASA, "Lunar Living: NASA's Artemis Base Camp Concept," NASA, 28 October 2020. [Online]. Available: <https://blogs.nasa.gov/artemis/2020/10/28/lunar-living-nasas-artemis-base-camp-concept/>. [Accessed December 2022].
- [24] A. Daga, M. Daga and W. Wendell, "A preliminary assessment of the potential of lava tube-situated lunar base architecture," in *SPACE 90 engineering, construction, and operations in space, Proceedings of the ASCE*, New York, 1990.

- [25] M. Vanderbilt, M. Criswell and W. Sadeh, "Structures for a lunar base," in *SPACE 88 engineering, construction, and operations in space, in: Proceedings of the ASCE*, New York, 1988.
- [26] P. Nowak, M. Criswell and W. Sadeh, "Inflatable structures for a lunar base," in *SPACE 90 engineering, construction, and operations in space, in: Proceedings of the ASCE*, New York, 1990.
- [27] P. Nowak, W. Sadeh and M. Criswell, "An analysis of an inflatable module for planetary surfaces," in *SPACE 92 engineering, construction, and operations in space, in: Proceedings of the ASCE*, New York, 1992.
- [28] W. Broad, "Lab Offers to Develop an Inflatable Space Base," *The New York Times*, 1989.
- [29] W. Sadeh and M. Criswell, "A generic inflatable structure for a lunar/martian base," in *SPACE 94 engineering, construction, and operations in space, in: Proceedings of the ASCE*, New York, 1994.
- [30] M. Criswell, W. Sadeh and J. Abarbanel, "Design and performance criteria for inflatable structures in space," in *SPACE 96, engineering, construction, and operations in space, in: Proceedings of the ASCE*, New York, 1996.
- [31] C. King, A. Butterfield, W. Hyper and J. Nealy, "A concept for using the external tank from a NSTS for a lunar habitat," in *Proceedings of the Ninth Biennial SSI/Princeton Conference on Space Manufacturing*, Princeton, 1989.
- [32] H. Benaroyaa and L. Bernold, "Engineering of lunar bases," *Acta Aeronautica*, vol. 62, pp. 277-299, 2008.
- [33] C. Purrington, G. Sowers and C. Dreyer, "Thermal Mining of volatiles in lunar regolith simulant," *Planetary and Space Science*, vol. 222, no. 105550, 2022.
- [34] H. Song, "Investigation on in-situ water ice recovery considering energy efficiency at the lunar south pole," *Applied Energy*, vol. 298, no. 117136, 2021.
- [35] A. Ogishima and K. Saiki, "Development of a micro-ice production apparatus and NIR spectral measurements of frosted minerals for future lunar ice exploration missions," *Icarus*, vol. 357, no. 114273, 2021.
- [36] B. Mckeown, A. Dempster, S. Saydam and J. Coulton, "Commercial Lunar Ice Mining: Is There a Role for Royalties?," *Space Policy*, 2022.
- [37] T. Sun, "Hydrogen ice within lunar polar craters," *International Journal of Hydrogen Energy*, vol. 47, pp. 34825-34840, 2022.

- [38] P. J. Godin, J. I. Kloos, A. Seguin and J. E. Moores, "Laboratory investigations of Lunar ice imaging in permanently shadowed regions using reflected starlight," *Acta Astronautica*, vol. 177, pp. 604-610, 2020.
- [39] "Possible Origin of Lunar Ice," *Advancements in Space Research*, vol. 30, pp. 1875-1881, 2002.
- [40] F. Sohl and G. Schubert, "Interior Structure, Composition, and Minerology of the Terrestrial Planets," in *Treatise on Geophysics*, Elsevier B.V., 2007, pp. 27-68.
- [41] D. McKay and D. Ming, "Properties of Lunar Regolith," *Developments in Soil Science*, vol. 19, pp. 449-462, 1990.
- [42] M. M. Monkul and A. Dacic, "Effect of grain size distribution on stress-strain behavior of lunar soil simulants," *Advances in Space Research*, vol. 60, pp. 636-651, 2017.
- [43] L. Keller and D. McKay, "The nature and origin of rims on lunar soil grains," *Geochimica et Cosmochimica Acta*, vol. 61, pp. 2331-2341, 1997.
- [44] G. Taylor, L. Martel, P. Lucey, J. Gillis-Davis, D. Blake and P. Sarrazin, "Modal analyses of lunar soils by quantitative X-ray diffraction analysis," *Geochimica et Cosmochimica Acta*, vol. 266, pp. 17-28, 2019.
- [45] E. Stansbery, "Lunar Rocks and Soils from Apollo Missions," ARES Developers, 31 March 2022. [Online]. Available: <https://curator.jsc.nasa.gov/lunar/>. [Accessed November 2022].
- [46] Y. C. Toklu and P. Akpınar, "Lunar soils, simulants and lunar construction materials: An overview," *Advances in Space Research*, vol. 70, pp. 762-779, 2022.
- [47] NASA, September 2006. [Online]. Available: <https://ntrs.nasa.gov/api/citations/20060051776/downloads/20060051776.pdf>. [Accessed 11 April 2023].
- [48] D. McKay, J. Carter, W. Boles and C. A. J. Allen, "JSC-1: A New Lunar Soil Simulant," *Engineering, Construction, and Operations in Space IV American Society of Civil Engineers*, pp. 857-866, 1994.
- [49] G. Just, K. Joy, M. Roy and K. Smith, "Geotechnical characterisation of two new low-fidelity lunar regolith analogues (UoM-B and UoM-W) for use in large-scale engineering experiments," *Acta Astronautica*, vol. 173, pp. 414-424, 2020.
- [50] L. Taylor, C. Pieters and D. Britt, "Evaluations of lunar regolith simulants," *Planetary and Space Sciences*, vol. 126, pp. 1-7, 2016.

- [51] C. Schrader, D. Rickman, C. McLemore, J. Fikes, D. Stoesser, S. Wentworth and D. McKay, "Lunar Regolith Characterization for Simulant Design and Evaluation Using Figure of Merit Algorithms," in *47th AIAA Aerospace Sciences Meeting Including The New Horizons Forum and Aerospace Exposition*, Orlando, FL, 2009.
- [52] P. Zarzycki and J. Katzer, "Multivariate Comparison of Lunar Soil Simulants," *Journal of Aerospace Engineering*, vol. 32, no. 5, 2019.
- [53] Exolith Labs, "Lunar Highlands (LHS-1) High-Fidelity Moon Dirt Simulant," Shopify, 2023. [Online]. Available: <https://exolithsimulants.com/products/lhs-1-lunar-highlands-simulant>. [Accessed March 2023].
- [54] P. Reiss, L. Grill and S. Barber, "Thermal extraction of volatiles from the lunar regolith simulant NU-LHT-2M: Preparations for in-situ analyses on the Moon," *Planetary and Space Science*, vol. 175, pp. 41-51, 2019.
- [55] L. Grill, P. Ostermeier, M. Wurth and P. Reiss, "Behaviour of lunar regolith simulants in fluidised bed reactors for in-situ resource utilisation," *Planetary and Space Science*, vol. 180, no. 104757, 2020.
- [56] C. Zhou, R. Chen, J. Xu, L. Ding, H. Luo, J. Fan, E. Chen, L. Cai and B. Tang, "In-situ construction method for lunar habitation: Chinese Super Mason," *Automation in Construction*, vol. 104, pp. 66-79, 2019.
- [57] C. Zhou, B. Tang, L. Ding, P. Sekula, Y. Zhou and Z. Zhang, "Design and automated assembly of Planetary LEGO Brick for lunar in-situ construction," *Automation in Construction*, vol. 118, no. 103282, 2020.
- [58] M. Isachenkov, S. Chugunov, I. Akhatov and I. Shishkovsky, "Regolith-based additive manufacturing for sustainable development of lunar infrastructure – An overview," *Acta Astronautica*, vol. 180, pp. 650-678, 2021.
- [59] A. Altun, F. Ertl, M. Marechal, A. Makaya, A. Sgambati and M. Schwentenwein, "Additive manufacturing of lunar regolith structures," *Open Ceramics*, p. 100058, 2021.
- [60] B. Lehner, D. Mazzotta, L. Teeney, F. Spina, A. Filosa, A. Canals Pou, A. Schlechten, S. Campbell and P. Lopez Soriano, "Human Assisted Robotic Vehicle Studies - A conceptual end-to-end mission architecture," *Radiation Measurements*, vol. 132, pp. 380-387, 2017.
- [61] A. Meurisse, C. Cazzaniga, C. Frost, A. Barnes, A. Makaya and M. Sperl, "Neutron radiation shielding with sintered lunar regolith," *Radiation Measurements*, vol. 132, no. 106247, 2020.
- [62] A. Lauermannova, I. Faltysova, M. Lojka, F. Antoncik, D. Sedmidubsky, Z. Pavlik, M. Pavlikova, M. Zaleska, A. Pivak and O. Jankovsky, "Regolith-based magnesium

- oxychloride composites doped by graphene: Novel high-performance building materials for lunar constructions," *FlatChem*, vol. 26, no. 100234, 2021.
- [63] NASA, "Ice on the Moon," 31 January 2022. [Online]. Available: https://nssdc.gsfc.nasa.gov/planetary/ice/ice_moon.html. [Accessed May 2023].
- [64] Y. Chen, T. Hwang, M. M. and J. Williams, "Mechanically activated carbothermic reduction of ilmenite," *Metallurgical and Material Transactions A*, vol. 28, pp. 1115-1121, 1997.
- [65] L. Sibille, D. Sadoway, S. Sirk, P. Tripathy, O. Melendez, E. Standish, J. Dominguez, D. Stefanescu, P. Curreri and S. Poizeau, "Recent Advances in Scale-Up Development of Molten Regolith Electrolysis for Oxygen Production in Support of a Lunar Base," in *47th AIAA Aerospace Sciences Meeting Including the New Horizons Forum and Aerospace Exposition*, 2012, Orlando.
- [66] Y. Yao, L. Wang, X. Zhu, W. Tu, Y. Zhou, R. Liu, J. Sun, B. Tao, C. Wang, X. Yu, L. Gao, Y. Cao, B. Wang, Z. Li, W. Yao, Y. Xiong, M. Yang, W. Wang and Z. Zou, "Extraterrestrial photosynthesis by Chang'E-5 lunar soil," *Joule*, vol. 6, no. 5, pp. 1008-1014, 2022.
- [67] R. Volger, G. Pettersson, S. Brouns, L. Rothschild, A. Cowley and B. Lehner, "Mining moon & mars with microbes: Biological approaches to extract iron from Lunar and Martian regolith," *Planetary and Space Science*, vol. 184, no. 104850, 2020.
- [68] F. J. Guerrero-Gonzalez and P. Zabel, "System Analysis of an ISRU Production Plant: Extraction of Metals and Oxygen from Lunar Regolith," *Acta Astronautica*, 2022.
- [69] S. J. Indyk and H. Benaroya, "A structural assessment of unrefined sintered lunar regolith simulant," *Acta Astronautica*, vol. 140, pp. 517-536, 2017.
- [70] C. H. Simonds, "Sintering and hot pressing of Fra Mauro composition glass and the lithification of lunar breccias," *American Journal of Science*, vol. 273, no. 5, pp. 428-439, 1973.
- [71] T. Gualtieri and A. Bandyopadhyay, "Compressive deformation of porous lunar regolith," *Materials Letters*, vol. 143, pp. 276-278, 2015.
- [72] T. Hoshino, S. Wakabayashi, S. Yoshihara and N. Hatanaka, "Key Technology Development for Future Lunar Utilization— Block Production Using Lunar Regolith," *Aerospace Technology Japan*, vol. 14, no. 30, pp. 35-40, 2016.

- [73] H. Benaroya, L. Bernold, J. Connoly, M. Duke, H. A. Franklin, S. Johnson and S. Matsumoto, "Workshop on Using In Situ Resources for Construction of Planetary Outposts," Lunar and Planetary Institute, Houston, 1998.
- [74] D. Rickman, E. J. and M. C., "Functional comparison of lunar regoliths and their simulants," *Journal of Aerospace Engineering*, vol. 26, pp. 176-182, 2013.
- [75] K. W. Farries, P. Visintin, S. T. Smith and P. van Eyk, "Sintered or melted regolith for lunar construction: state-of-the-art review and future research directions," *Construction and Building Materials*, vol. 296, no. 123627, 2021.
- [76] A. Meurisse, J. C. Beltzung, M. Kolbe and A. Cowley, "Influence of Mineral Composition on Sintering Lunar Regolith," *Journal of Aerospace Engineering*, vol. 30, no. 4, 2017.
- [77] International Code Council, "Strength of Concrete," 2012. [Online]. [Accessed May 2023].
- [78] E. Cardiff, B. Hall and N. GSFC, "A Dust Mitigation Vehicle Utilizing Direct Solar Heating," University of Maryland, College Park, 2008.
- [79] P. Hintze, J. Curran and T. Back, "Lunar Surface Stabilization via Sintering or the Use of Heat Cured Polymers," in *47th AIAA Aerospace Science Meeting*, Orlando, 2009.
- [80] L. A. Taylor and T. T. Meek, "Microwave Sintering of Lunar Soil: Properties, Theory, and Practice," *Journal of Aerospace Engineering*, vol. 18, no. 3, 2005.
- [81] V. Srivastava, S. Lim and M. Anand, "Microwave processing of lunar soil for supporting longer-term surface exploration on the Moon," *Space Policy*, vol. 37, pp. 92-96, 2016.
- [82] S. Gholami, X. Zhang, Y.-J. Kim, Y.-R. Kim, B. Cui, H.-S. Shin and J. Lee, "Hybrid microwave sintering of a lunar soil simulant: Effects of processing parameters on microstructure characteristics and mechanical properties," *Materials Design*, vol. 220, no. 110878, 2022.
- [83] T. Nakamura and B. Smith, "Solar thermal system for lunar ISRU applications: development and field operation at Mauna Kea, HI," *Nonimaging Opt. Effic. Des. Illum. Sol. Conc. VIII*, no. 8124, 2011.
- [84] A. S. Howe, B. Wilcox, M. Barmatz and G. Voecks, "ATHLETE as a Mobile ISRU and Regolith Construction Platform," California Institute of Technology, Pasadena, 2016.
- [85] A. Meurisse, A. Makaya, C. Willsch and M. Sperl, "Solar 3D printing of lunar regolith," *Acta Astronautica*, vol. 152, pp. 800-810, 2018.

- [86] Y.-J. Kim, B. H. Ryu, H. Jin, J. Lee and H.-S. Shin, "Microstructural, mechanical, and thermal properties of microwave-sintered KLS-1 lunar regolith simulant," *Ceramics International*, vol. 47, no. 19, pp. 26891-26897, 2021.
- [87] X. Zhang, S. Gholami, M. Khedmati, B. Cui, Y.-R. Kim, Y.-J. Kim, H.-S. Shin and J. Lee, "Spark plasma sintering of a lunar regolith simulant: effects of parameters on microstructure evolution, phase transformation, and mechanical properties," *Ceramics International*, vol. 47, no. 4, pp. 5209-5220, 2021.
- [88] ASTM, "Standard Test Methods for Sampling and Testing Brick and Structural Clay Tile," ASTM, 22 June 2021. [Online]. Available: https://www.astm.org/c0067_c0067m-21.html. [Accessed December 2022].
- [89] T. Alam, "Compressive Strength of Brick," *CivilToday*, [Online]. Available: <https://civiltoday.com/civil-engineering-materials/brick/137-compressive-strength-of-brick>. [Accessed December 2022].
- [90] K. Kim and F. Milstein, "Relation between hardness and compressive strength of polymer concrete," *Construction and Building Materials*, vol. 1, no. 4, pp. 209-214, 1987.
- [91] T. E. S. Agency, "Building a Lunar Base with 3D Printing," The European Space Agency, 31 January 2013. [Online]. Available: https://www.esa.int/Enabling_Support/Space_Engineering_Technology/Building_a_lunar_base_with_3D_printing. [Accessed December 2022].
- [92] D. Zhang, D. Zhou, G. Zhang and G. L. L. Shao, "3D printing lunar architecture with a novel cable-driven printer," *Acta Astronautica*, vol. 189, pp. 671-678, 2021.
- [93] D. Urbina, H. Madakashira, J. Salini, S. Govindaraj, R. Bjoerstad, J. Gancet, M. Sperl, A. Meurisse, M. Fateri and B. Imhof, "Robotic prototypes for the solar sintering of regolith on the lunar surface developed within the Regolight project," in *68th International Astronautical Congress*, Adelaide, 2017.
- [94] J. M. Hickman, H. B. Curtis and G. A. Landis, "Design Considerations for Lunar Base Photovoltaic Power Systems," 21 May 1990. [Online]. Available: <https://ntrs.nasa.gov/api/citations/19910004946/downloads/19910004946.pdf>. [Accessed December 2022].
- [95] W. Rogers and S. Sture, "Indigenous lunar construction materials," in *Centre for Space Construction Third Annual Symposium*, 1991.
- [96] G. Hammond and C. Jones, "Embodied energy and carbon in construction materials," in *Proceedings of the Institution of Civil Engineers-Energy*, 2008.

- [97] V. Krishna Balla, L. B. Roberson, G. W. O'Connor, S. Trigwell, S. Bose and A. Bandyopadhyay, "First demonstration on direct laser fabrication of lunar regolith parts," *Rapid Prototyping Journal*, vol. 18, no. 6, 2012.
- [98] N. Gerdes, L. Fokken, S. Linke, S. Kaierle, O. Suttmann, J. Hermsdorf, E. Stoll and C. Trentlage, "Selective Laser Melting for processing of regolith in support of a lunar base," *Journal of Laser Applications*, vol. 30, no. 032018, 2018.
- [99] Y. Ishikawa, T. Sasaki and T. Higasayama, "Simple and efficient methods to produce construction materials for lunar and Mars bases," in *Engineering, Construction and Operations in Space III*, Denver, 1992.
- [100] S. Allan, B. Merritt, B. Griffin, P. Hintze and H. Shulman, "Hightemperature microwave dielectric properties and processing of JSC-1AC lunar simulant," *Journal of Aerospace Engineering*, vol. 26, p. 874–881, 2013.
- [101] R. Mueller, L. Sibille, P. Hintze, T. Lippitt, J. Mantovani, M. Nugent and I. Townsend, "Additive Construction using Basalt Regolith Fines, Earth and Space: Engineering for Extreme Environments," in *Proceedings of the 14th Biennial ASCE Conference on Engineering*, St. Louis, 2014.
- [102] G. Hammond and C. Jones, "Embodied energy and carbon in construction materials," in *Proceedings of the Institution of Civil Engineers-Energy*, 2008.
- [103] S. A. Howe, B. H. Wilcox, C. McQuin, J. Townsen, R. R. Rieber, M. Barmatz and J. Leichty, "Faxing Structures to the Moon: Freeform Additive Construction System (FACS)," in *AIAA*, 2013.
- [104] W. Rogers and S. Sture, "Indigenous lunar construction materials," in *Centre for Space Construction Third Annual Symposium*, 1991.
- [105] S. Frazier, "NASA, ICON Advance Lunar Construction Technology for Moon Missions," NASA, 29 November 2022. [Online]. Available: <https://www.nasa.gov/press-release/nasa-icon-advance-lunar-construction-technology-for-moon-missions>. [Accessed December 2022].
- [106] N. Woolf and R. Angel, "Pantheon habitat made from regolith, with a focusing solar reflector," *Philosophical Transactions of the Royal Society A*, vol. 379, no. 2188, 2020.
- [107] 3DWasp, "3d printed house tecla," Worlds Advanced Saving Project, [Online]. Available: <https://www.3dwasp.com/en/3d-printed-house-tecla/>. [Accessed January 2023].

- [108] R. Buswell, W. Leal de Silva, S. Jones and J. Dirrenberger, "3D printing using concrete extrusion: A roadmap for research," *Cement and Concrete Research*, vol. 112, pp. 37-49, 2018.
- [109] C. Allen, J. Hines, D. McKay and R. Morris, "Sintering of Lunar Glass and Basalt," in *Engineering, Construction, and Operations in Space III*, Denver, CO, 1992.
- [110] C. Allen, "Bricks and ceramics," Lunar and Planetary Institute, Albuquerque, NM, 1998.
- [111] M. Fateri, A. Cowley, M. Kolbe, O. Garcia, M. Sperl and S. Cristoforetti, "Localized Microwave Thermal Posttreatment of Sintered Samples of Lunar Simulant," *Journal of Aerospace Engineering*, vol. 32, no. 04019051, 2019.
- [112] M. Fateri, A. Meurisse, M. Sperl, D. Urbina, H. Madakashira, S. Govindaraj, J. Gancet, B. Imhof, W. Hoheneder, R. Waclavicek, C. Preisinger, E. Podreka, M. Mohamed and P. Weiss, "Solar Sintering for Lunar Additive Manufacturing," *Journal of Aerospace Engineering*, vol. 32, no. 4019101, 2019.
- [113] K. Cowing, "Using a Planetary Analog To Test a Prototype Inflated Habitat for NASA," SpaceRef, 18 November 2007. [Online]. Available: <https://spaceref.com/uncategorized/using-a-planetary-analog-to-test-a-prototype-inflated-habitat-for-nasa/>. [Accessed December 2022].
- [114] European Space Agency, "Spaceship EAC," European Space Agency, 12 August 2021. [Online]. [Accessed May 2023].

BIOGRAPHY OF THE AUTHOR

Thomas Cox was born in Rockport, Maine on November 16, 1997. He was raised in Appleton, Maine and graduated from Camden Hills Regional High School in 2016. He attended the University of Maine and graduated in 2020 with a Bachelor's degree in Mechanical Engineering. He immediately entered the Mechanical Engineering graduate program in the Summer of 2020. After receiving his degree, Thomas will begin his career as a mechanical engineer. Thomas is a candidate for the Master of Science degree in Mechanical Engineering from the University of Maine in May 2023.